TALLINN UNIVERSITY OF TECHNOLOGY
SCHOOL OF ENGINEERING

Department of Civil Engineering and Architecture

EXPERIMENTAL STUDY OF CO_2 MINERALIZATION IN BURNT OIL SHALE AND CEMENT BYPASS DUST BASED SYSTEMS

SÜSINIKDIOKSIIDI MINERALISEERIMISPROTSESSI UURIMINE PÕLEVKIVI- NING TSEMENDITÖÖSTUSE JÄÄTMETEL PÕHINEVATES SÜSTEEMIDES

MASTER THESIS

Student	Mustafa Cem Usta
Student code	177351
Supervisor	Dr. Can Rüştü Yörük
Co-supervisor	Dr. Mai Uibu

Tallinn, 2019

TALLINNA TEHNIKAÜLIKOOL
INSENERITEADUSKOND

Ehituse ja arhitektuuri instituut

SÜSINIKDIOKSIIDI MINERALISEERIMISPROTSESSI UURIMINE PÕLEVKIVI- NING TSEMENDITÖÖSTUSE JÄÄTMETEL PÕHINEVATES SÜSTEEMIDES

EXPERIMENTAL STUDY OF CO_2 MINERALIZATION IN BURNT OIL SHALE AND CEMENT BYPASS DUST BASED SYSTEMS

MAGISTRITÖÖ

Üliõpilane:	Mustafa Cem Usta
Üliõpilaskood:	177351
Juhendaja:	Dr. Can Rüştü Yörük
Kaasjuhendaja:	Dr. Mai Uibu

Tallinn, 2019

AUTHOR’S DECLARATION

Hereby I declare, that I have written this thesis independently.
No academic degree has been applied for based on this material.
All works, major viewpoints and data of the other authors used in this thesis have been referenced.

“.......” .... 201…..

Author: ....
/signature /

Thesis is in accordance with terms and requirements

“.......” .... 201….

Supervisor: …..........................
/signature/

Accepted for defence

“.......”....................201… .

Chairman of theses defence commission: ....
/name and signature/

Department of Civil Engineering and Architecture

THESIS TASK

Student: Mustafa Cem Usta 177351EABM

Study programme: EABM - Environmental Engineering and Management

Supervisors: Engineer - Dr. Can Rüştü Yörük Phone: +37258542373
Senior Research Scientist – Dr. Mai Uibu Phone: +3726202812

Thesis topic:
(in English): Experimental study of CO_2 mineralization in burnt oil shale and cement bypass dust based systems

(in Estonian) Süsinikdioksiidi mineraliseerimisprotsessi uurimine põlevkivi- ning tsemenditööstuse jäätmetel põhinevates süsteemides

Thesis main objectives:

1. Literature review
2. Laboratory mineral carbonation experiments
3. Analyzing results
4. Thesis finalization

Thesis tasks and time schedule:

No	Task description	Deadline
1.	Literature review	1 March 2019
2.	Laboratory mineral carbonation experiments	30 March 2019
3.	Analyzing results	30 April 2019
4.	Thesis finalization	21 May 2019

Language: English **Deadline for submission of thesis:** 23 May 2019

Student: Mustafa Cem Usta ....201....
/signature/

Supervisor: Dr. Can Rüştü Yörük ....201....
/signature/

Consultant: Dr. Mai Uibu ....201....
/signature/

ACKNOWLEDGEMENT

This master’s thesis is based on research done from October 2018 to May 2019 in the Laboratory of Inorganic Materials at Tallinn University of Technology under the guidance of Dr. Can Rüştü Yörük and Dr. Mai Uibu. It is carried out as a part of HORIZON 2020 project Clean clinker production by Calcium looping process (CLEANKER). This project has received funding from the European Union's Horizon 2020 Framework Programme under Grant Agreement n. 764816. This work is also supported by the Chinese Government (National Natural Science Foundation of China) under contract No.91434124 and No.51376105 and by institutional research funding IUT (IUT33-19) of the Estonian Ministry of Education and Research.

I would like to thank Prof. Andres Trikkel and Prof. Rein Kuusik for giving me the opportunity to write my master’s thesis in the laboratory. I thank especially my supervisor Dr. Can Rüştü Yörük for his valuable comments and contributions throughout the learning process of this thesis. Furthermore, I would like to thank Dr. Mai Uibu for her supports in the laboratory analysis and for her valuable comments on my master’s thesis. I would also like to thank all members of the Laboratory of Inorganic Materials for being very friendly and helpful. Last but not least, I wish to thank my family and my partner Nawal for supporting and encouraging me not only during this project, but throughout my studies as well.

Tallinn, May 13th, 2019

Mustafa Cem Usta

Table of Contents

List of Figures

List of Tables

List of Abbreviations

2DS	2 Degree Scenario
APC	Air Pollution Control
BET	Brunauer Emmett Teller
BOS	Burnt Oil Shale
BPD	Bypass Dust
CaL	Calcium Looping
CBPD	Cement Bypass Dust
CCS	Carbon Capture and Storage
CKD	Cement Kiln Dust
FT-IR	Fourier Transform Infrared Spectroscopy
GHG	Greenhouse Gases
IEA	International Energy Agency
ISSA	Incinerator Sewage Sludge Ash
OPC	Ordinary Portland Cement
OS	Oil Shale
PPM	Particles Per Million
RCA	Recycled Concrete Aggregate
RTS	Reference Technology Scenario
SSA	Specific Surface Area
TGA	Thermogravimetric Analysis
UC	Uptake Capacity

1.INTRODUCTION

1.1 General background

Presently, 80 percent of the world's energy supply is dependent on fossil carbons, such as coal, oil shale (OS), peat, liquid oil and natural gas [1]. These fuels are non-renewable sources of energy that are expended at a rate greater than the rate at which they are produced in nature. The exploitation of fossil fuels for industrial and home uses results in environmentally unsafe disposal or reuse of solid waste (especially low-grade solid fuels), the atmospheric emissions of Carbon Dioxide (CO_2) and the production of other greenhouse gases (GHG) that have deleterious effects on human health and the planet's environment. One of the sectors that emits considerable amount of CO_2 emissions to the atmosphere is the cement sector. Cement is the second most-consumed resource in the world, with greater than 4 billion tons of the material produced globally every year [2]. According to Olivier and his colleagues cement industry is responsible for about 8% of the global anthropogenic CO_2 emissions [3]. In state-of-the-art dry clinker burning processes, CO_2 produced from $CaCO_3$ calcination constitutes about 60% of the total CO_2 emissions, while the remaining percentages are being emitted from fossil fuel combustion [4]. The fifth report of Intergovernmental Panel on Climate Change also reveals that the noteworthy increments of GHG in the atmosphere since the beginning of industrial period are an aftereffect of human consumption of non-renewable energy sources and different chemical procedures [5].

The International Energy Agency (2017) further predicts that fossil fuels will continue to be the dominant source of energy production for the next few decades across the world. A report by United Nations Population Fund (UNFPA) estimates that in 2018 the global population was roughly 7.6 billion and is expected to rise by 29 percent (an additional 2.3 billion people) in the next 32 years, reaching a global population of 9.9 billion by 2050 [6]. This population rise is expected to increase the demands of energy production and consumption, and increase demands in the construction and cement sectors across the Earth. The World Energy Report (2017) predicts that by 2040 energy demands are expected to increase by over 30 percent [7]. Figure 1 represents these expectations on overall energy consumption around the world from different fuel sources. It demonstrates that petroleum products are projected to stay as the predominant source of energy consumption and represent over 74 percent of absolute energy consumption in use by 2040 [7].

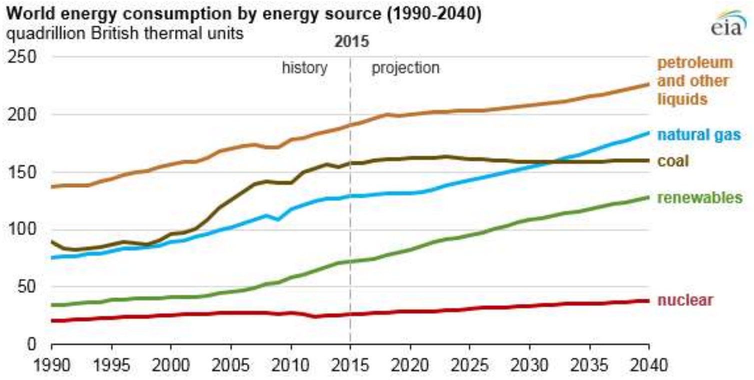

Figure 1. Energy consumption by fuel source [7]

If energy consumption by fuel source continues to be dominated by fossil fuels as the data in Figure 1 predicts, the utilization of these fuels will prompt a rise in solid wastes and GHG emissions. It is imperative that the world switches to greener and more sustainable sources of energy production that do not have harmful environmental consequences. However, the transition to cleaner and greener energy is a slow process marked by complex economic and political considerations. This means that the immediate environmental risks associated with fossil fuels need to be mitigated. The two key challenges for our time are thus; devising effective methods to dispose of solid wastes generated by fossil fuels and controlling the atmospheric emissions of GHG such as CO_2.

A key intervention can be made in the cement industry. Cement is a binding material that has been used for buildings since ancient Rome. The biggest CO_2 emission from decomposition of carbonates today comes from cement industry. 20th century's global industrialization has caused the cement industry to grow rapidly, with current levels of global production equivalent to more than half a ton per person per year, as can be seen in Figure 2. Global cement production has increased more than 30-fold since 1950 and almost 4-fold since 1990, with more marked growth than global fossil energy production in the last 2 decades. Since 1990 this growth has largely been because of rapid development in China where cement production has grown by a factor of almost 12 such that 73 % of global growth in cement production since 1990 has occurred in China [8,9]. This exponential growth in production has added extra strain on Earth's ability to cope with anthropogenic CO_2 in the atmosphere.

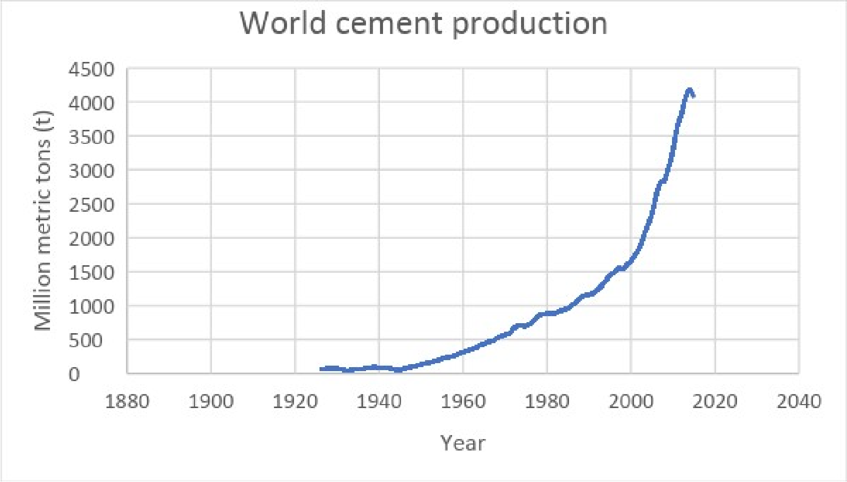

Figure 2 Global cement production [8]

The effects of the current levels of CO_2 in the atmosphere have already been felt through processes of global warming and climate change. This has caused concern among the scientific community that sees GHG as the most significant contributor to climate change and aims to curtail these emission levels so that global temperature change is fixed below 2.0 degrees by the year 2050 [10]. The future projected utilization of fossil fuels on an even larger scale will prompt the aggregation of CO_2 emissions in the atmosphere, considerably changing the Earth's climate by raising temperatures and increasing the probabilities of environmental catastrophes. It is therefore vital to explore avenues for the decrease in CO_2 emissions from fossil fuel- fired energy production, into the atmosphere.

1.2 Mechanisms to decrease CO_2 emissions

This decrease can be achieved in numerous ways. The development of sustainable power sources will be a priority particularly in Europe. There will also be a propensity to decrease the share of non-inexhaustible sources in primary energy production. During this transition period towards non-fossil energy (nuclear power and renewable forms of energy), the reduction of CO_2 discharges and relief from the negative outcomes of high atmospheric levels of CO_2 will be of extreme importance in curbing further climate change and environmental degradation [11]. There are numerous options available to achieve a sustainable reduction of CO_2 emissions, e.g. fuel switching to lower C/H ratios, improving energy efficiency, direct fuel gas cleaning, and a more through intensive implementation of Carbon Capture and Storage (CCS) technologies.

Interestingly, the Two-degree scenario (2DS) requires CO_2 emissions to peak before 2020 and to tumble to around one-quarter of 2014 levels by 2060 [10]. Alternatively, the reference technology scenario (RTS) requires the increase in CO_2 emissions to keep on slowing till 2060, when emissions would be 16% higher than 2014 levels, and come to nearly 40 $GtCO_2$. In this situation, the energy sector CO_2 emissions do not reach highest point until around 2050. The total carbon spending plan over the period to 2060 is about 40% lower during the 2DS in contrast to the RTS, requiring reduction of an extra 760 $GtCO_2$ over this period. Figure 3 demonstrates the conceivable advances for decreasing CO_2 emissions that are proposed in the report of International Energy Agency (IEA) Energy Technology Perspectives which provides an overview for both 2DS and RTS scenarios (2017) [12].

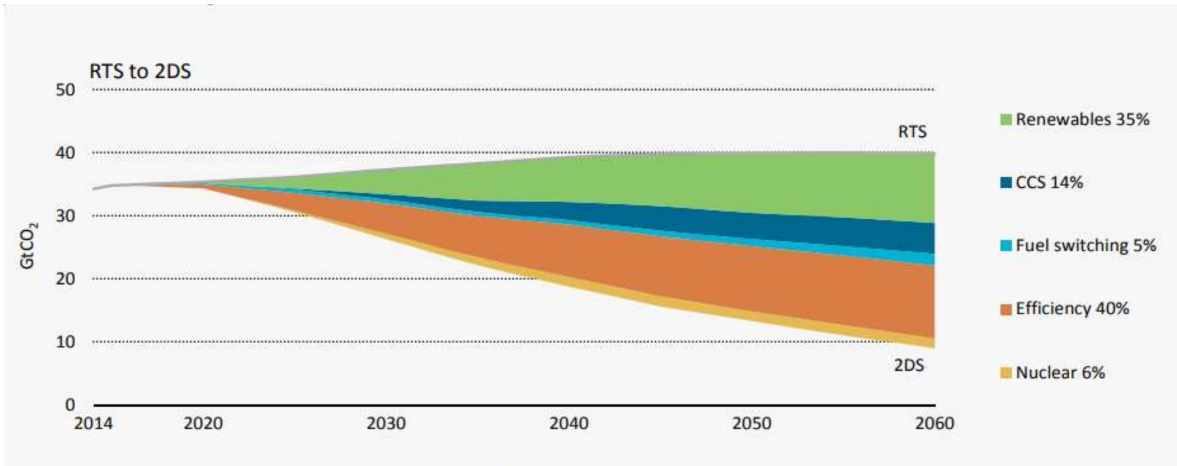

Note: CO_2 emissions include both energy-related CO_2 emissions and emissions from industrial processes.

Figure 3 Global CO_2 emissions reductions by technology [12]

This report provides a detailed overview of the wide and diverse range of energy efficient and low carbon innovations needed over all areas of the economy to achieve the desired CO_2 emissions decrease. A significant contribution to lowering current rates of CO_2 will be made by the switch towards renewable energy sources and increased efficiency, representing 35 percent and 40 percent shares respectively. Fuel switching and transitions to nuclear sources of energy will also contribute in limited quantities of 5 percent and 6 percent respectively. The report further demonstrates that Carbon Capture Systems and advanced procedures employing innovative storage techniques will contribute by over 14 percent in reducing global CO_2 emissions by 2060 [12].

CCS thus shows up as an emergent but key technology that needs to be improved rapidly for attaining substantial decreases in the current and rising CO_2 emissions produced from fossil fuel combustion and non-renewable energy sources.

1.3 Options for Estonia

Estonia is one of the countries utilizing low grade fossil fuel - OS as a primary energy source. Estonia is number one in energy independency among the EU member states because of its local OS deposits [13]. However, being dependent on fossil fuel as a primary energy source comes with a price. Estonia ranks as the first across the EU in CO_2 emission per kilowatt-hour [14]. Estonian OS is characterized by especially high specific carbon emissions (29.1 tC/TJ). Most of Estonian (95%) electricity and heat production is based on OS combustion which produces enormous amounts (~7 Mt annually) of calcareous ash, most of which is currently deposited in waste piles due to a lacking industrial application. The Estonian state has approved a strategy aimed at reducing emissions of GHG by 80% till 2050 in comparison with the emission levels of 1990 [15]. However, the current OS development plan 2016-2030 under operation in the country does not see a need for reducing mining quotas and currently produces close to a limit of 20 million tons which exceeds the recommended mining limits to minimize CO_2 release [16]. These trends tend to indicate that Estonia does not intend to change its source of the primary energy production in the near future. Therefore, it is imperative for Estonia to look for possible CCS solutions for emissions from OS energetics in order to achieve both national and EU targets of emission reduction.

Estonia does not have suitable geological conditions for carbon storage because of its geographical landscape; a shallow sedimentary basin and potable water in aquifers [17]. Therefore, one of the viable and promising CCS alternatives for Estonia is mineral carbonation of OS ash which is also abundantly available. Depending on the combustion technology, the ash contains from 10 to 25% free Ca and Mg oxides and are considered as CO_2 binder even under natural weathering conditions [18]. Recent developments involving ash water suspension carbonation demonstrated that OS ashes are able to bind up to 290 kg CO_2 per ton of ash [19]. An option for the utilization of OS ash stemming from its good binding properties can be seen in road construction since 1970s. Here ash has been used as a covering for dust control on the roads and in the building of the monolithic bases of the roads [20].

For these reasons the carbonation of OS ash generated in power plants can be a useful material as sorbent to utilize and stabilize the alkalinity of the OS ash with carbonation and further may minimize the leaching of trace elements which can come into existence in soil and soil organisms. Additionally, development goals of Estonia can be achieved in both economic and ecological perspectives. The product of OS ash carbonation process can also be considered as by-product that can further be re-used in construction aspects that eventually minimize negative environmental issues while closing the material loop, decreasing the usage of raw materials and supporting the emergence of a circular economy.

The general need to address rising CO_2 emissions and the specific emphasis on curbing the detrimental effects of fossil fuel-based energetics and cement industry, are the central focus of this thesis. This thesis draws insight from OS based energy sector of Estonia considering processed or burnt oi shale (BOS) wastes as sorbent for possible Calcium looping (CaL) applications and makes contributions with the gained experimental knowledge to the HORIZON 2020 CLEANKER project of clean clinker production by CaL process by exploring BOS and BPD as potential sources for mineral carbonation techniques of carbon capture and sequestration. The effects of hydration and grinding on mineral carbonation due to changes in SSA and CO_2 uptake potentials of industrial alkaline waste (BOS, BPD) in lower temperatures than 650 °C is discussed in detail in this thesis work.

This thesis thus seeks to contribute to the development of those CO_2 capture and storage techniques which will utilize the waste residues from fossil fuels and cement industries by producing knowledge regarding CO_2 mineralization potentials and reaction kinetics of mineral carbonation with industrial alkaline wastes. The rest of this subsection will explore the need to pursue CCS in Estonia. The second chapter provides an overview of various CCS techniques and comprehensive literature review on mineral carbonation. The literature review specifically frames the background for mineral carbonation, explores the direct and indirect mineral carbonation technique, comments on the advantages/disadvantages of mineral carbonation. The chapter additionally explores carbonation of natural and industrial wastes and demonstrates that mineral carbonation is a useful technique for CCS utilizing oil shale ash and cement wastes. Drawing from the insights of the literature, chapter three presents an overview of the methods and methodology employed to investigate direct gas-solid carbonation of burnt oil shale and cement bypass dust. Chapter four presents the results and discussions of the experiments with particular focus on the role of temperature and pre-treatment of materials on carbonation. Chapter five provides the conclusion and reflects on the insights gained from the experiments. A summary is presented at the end of the conclusions, to provide a comprehensive overview of the research undertaken for the production of this thesis.

2. LITERATURE REVIEW

2.1 Background to carbon capture methods

There are numerous techniques and methods for carbon capture and sequestration. This subsection examines the predominant methods of carbon capture before detailing the basics of mineral carbonation which is the central focus of this thesis.

Scholes (2013) demonstrates that these three principal techniques for carbon capture: post-combustion, pre-combustion and oxy-fuel (OF) combustion [21]. Figure 4 details the main procedures related to these three unique but similar techniques.

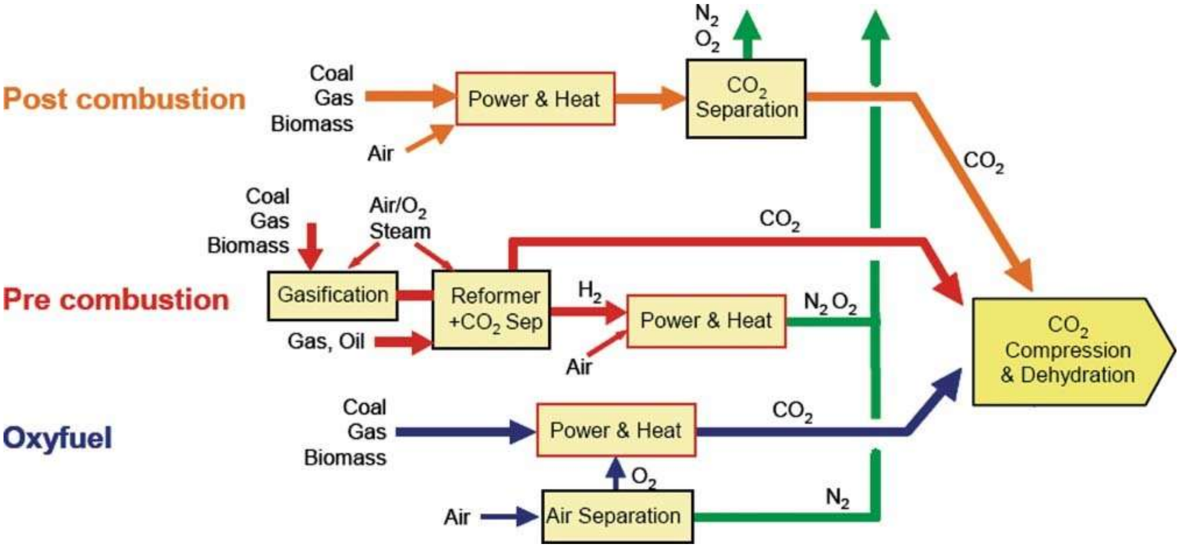

Figure 4 Three main categories of carbon capture technologies [22]

Post-combustion

In the post-combustion method, CO_2 is separated from the flue gas of the power station by passing the gas through an absorber column packed with liquid solvents (such as ammonia) that preferentially separate the CO_2. In the most commonly-used techniques, once the chemicals in the absorber column become saturated, a stream of superheated steam at around 120°C is passed through it. This releases the trapped CO_2, which can then be transported to storage facilities [23]. More experimental techniques to scrub CO_2 from flue gas without the two-step process include using seawater to absorb the gas and then returning the mixture back to the ocean for long-term storage [24].

Pre-combustion

This method is generally applied to coal-gasification combined cycle power plants. The coal is gasified to produce a synthetic gas made from carbon monoxide and hydrogen. The former is reacted with water to produce CO_2, which is captured, and more hydrogen. The hydrogen can be diverted to a turbine for electricity production. Alternatively, some of this gas can be bled off to feed hydrogen fuel cells for cars [25].

One disadvantage of the pre-combustion method is that it cannot be retro-fitted to the older pulverized coal power plants that make up much of the world's installed base of fossil fuel power. It could perhaps be used in natural gas stations, where a synthetic gas is first produced by producing reactions between the methane and the steam to produce carbon dioxide and hydrogen. However, the economic advantage of this method over post-combustion is yet to be proven.

Oxyfuel

When coal, oil or natural gas is burned conventionally, the amount of CO_2 produced is between 3-15% of the waste gases, depending on the fuel. Oxyfuel is an alternative CCS method that produces a highly concentrated stream of CO_2, easier for capture and storage. The oxyfuel combustion pathway is a process of burning fossil fuels with an oxygen-enriched flue gas mixture instead of air. In this environment, virtually all the waste gas tends to be composed of mainly CO_2 and water vapor. Where the former can be transported directly to the storage facility and the latter can be removed through condensation techniques and utilized elsewhere [26].

In the oxyfuel system, the air has to be separated into liquid oxygen, gaseous nitrogen, argon and other trace gases and this process can consume up to 15% of the power produced at the station [27]. The novel application of oxyfuel combustion technology to fossil-fuel energy conversion systems represents an emerging opportunity for the development of new concepts and designs, increasing the efficiency of the baseline combustion processes, and reducing their environmental footprints through CCS.

2.2 Alternative CCS methods

CCS has other potential application methods that can provide alternatives to geological storage, and help the world transition to a lower-carbon economy. These methods include chemical looping, calcium looping and mineral carbonation discussed below.

Chemical Looping

Chemical looping constitutes novel technology regarding sending oxygen that is separated from air to the process of coal conversion. This method ensures high concentration of CO_2 after combustion which does not need extra steps for capturing CO_2.

A metal or metal oxide reaction is employed to carry oxygen to combustion reactor (see Figure 5). Processes of oxidation occurs as metal particles are left in contact with air and produce metal oxides. This reaction imitates natural corrosion which happens in atmospheric conditions at lower rates.

This mechanism thus allows for the production of pure CO_2 flue gas which is ready for sequestration storage.

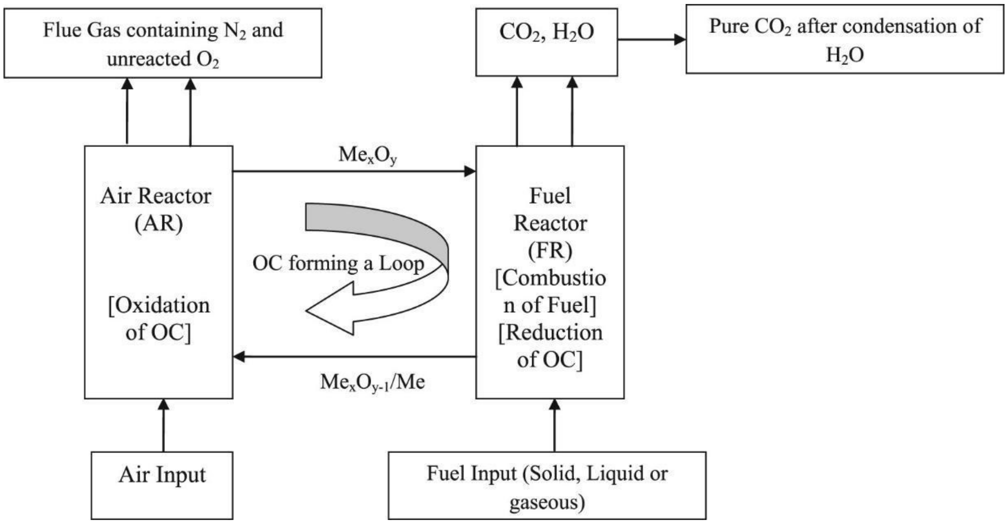

Figure 5 Line diagram depicting Chemical Looping Combustion (CLC) process [28].

Ca-Looping

Calcium Looping (CaL) is one more CO_2 capture innovation which has progressively been concentrated in CCS. The CaL concept was originally proposed by Shimizu et al (1999) and it is based on the reversible reaction between CaO and CO_2 at high temperature [25]. CO_2-rich gases come into contact with CaO-rich solids in the carbonator (see Figure 6) where an exothermic carbonation reaction occurs. Solids containing the $CaCO_3$ formed by the carbonation reaction are sent to a second reactor called calciner (as shown in Figure 6) for regeneration at a temperature of 920°C. The high temperatures required to withstand the calcination reaction in a CO_2-rich environment are guaranteed by the combustion of coal with an oxygen-rich mixture, which does not nullify carbon separation. The technique has been developed recently as a potentially low-cost technology for CO_2 capture. Therefore, CaL is one of the promising future CCS techniques that can help diminish the carbon emissions caused by the workings of different industries including energy, cement etc.

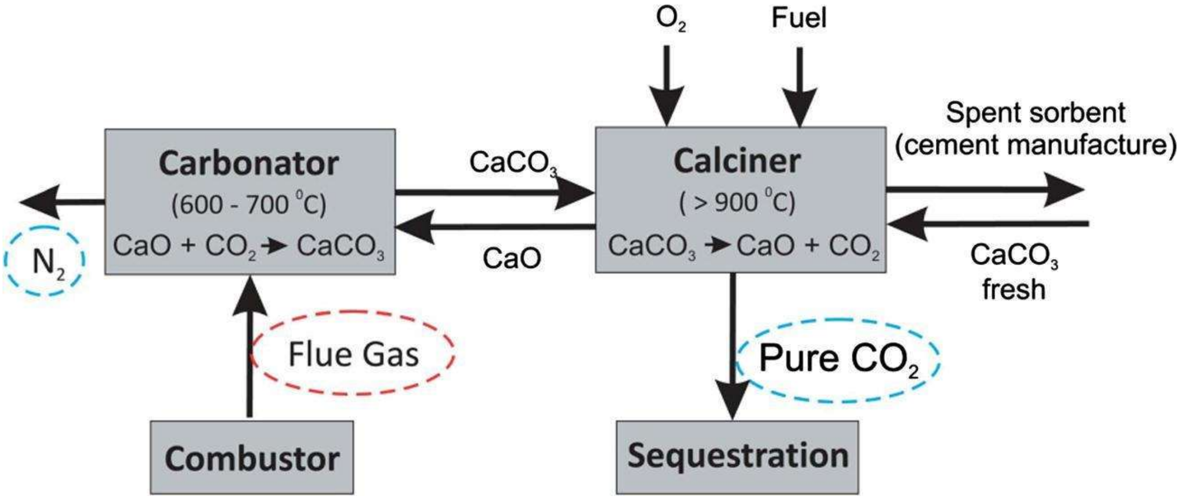

Figure 6 Schematic representation of the CaL process for CO_2 capture from post-combustion flue gas [29].

Mineral Carbonation

Another possible technology that can contribute to reductions in CO_2 atmospheric emissions is to sequester CO_2 into minerals that are naturally occurring or produced as a waste by industry. As mineral carbonation is the focus of the thesis, a detailed analysis of the basic principle behind mineral carbonation, the techniques of carbonation and its potential advantages/disadvantages are discussed below.

2.3 A detailed look at mineral carbonation

The basics of Mineral Carbonation

Mineral carbonation is usually undertaken to mimic the naturally occurring weathering reaction which is a process that includes utilizing calcium and magnesium minerals on the Earth’s crust, and forming solid carbonates by capturing gaseous CO_2 from atmosphere as demonstrated by the chemical reaction below.

$$(Ca,Mg)SiO_3\,(s) + CO_2\,(g) \rightarrow (Ca,Mg)CO_3\,(s) + SiO_2\,(s) \qquad (1)$$

The mineral carbonation (Eq. 1) prevalent in nature is a very slow reaction that can take thousands of years. Since human activity increased rate of carbon emission, carbonation needs to occur in order of minutes to be effective for environmental regulation and industrial implementation. Mineral carbonation can be done by using natural minerals such as wollastonite, serpentine or olivine which are abundant around the world. In addition to natural minerals, industrial waste residues like slags and combustion ashes can also be used in the same purpose for CO_2 sequestration.

Although natural minerals have huge capacity and availability around the world, the mining, transport, pre-treatment of ore and the extreme operating conditions tend to increase the processing costs and the energy demands required to undertake mineral carbonation. However, mineralization of waste residues is likely to be less costly since the waste is generated close to CO_2 emission sources and therefore incurs no additional transportation or mining costs for mineral carbonation processes. Therefore, thermodynamic stabilization of waste material while storing CO_2 is more sustainable compared to the usage of natural minerals. The carbonated product might have a commercial value and can be reused in construction or mining industry. Closing the material loop while achieving thermodynamically stable storage of CO_2 is the most desirable option in mineral carbonation. Figure 7 shows a schematic drawing of a mineral CO_2 sequestration process on the basis of both ore and industrial residue carbonation. [30]

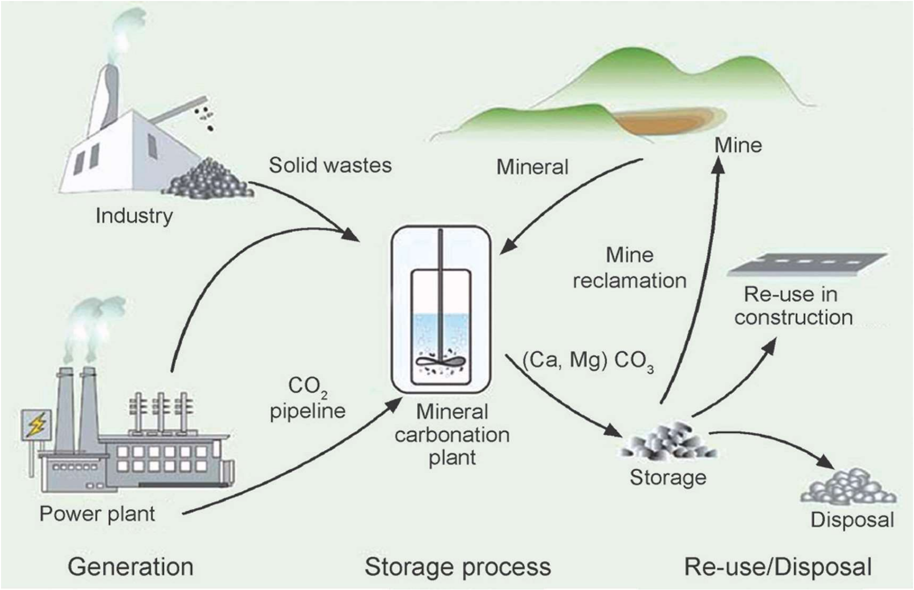

Figure 7 Schematic drawing of a mineral CO_2 sequestration process. [30]

Mineral Carbonation Background

Mineral carbonation is a relatively new idea emerging in the early 90s in CCS technologies that aimed to mitigate CO_2 emissions. Seifritz first described it in 1990 as a binding method for CO_2 [31]. This was further explained by Dusmore in 1992 who added studies related CO_2 binding possibilities of calcium and magnesium bearing minerals [32]. Lackner et al further expanded these studies in 1995 establishing silicate minerals (olivine, serpentine and wollastonite) and also basalt rock as the most suitable natural raw materials that are both cheap and abundant in the world. His contributions paved the way for an acceleration of the research in this field and established mineral carbonation as a viable technique that is still utilized in present day research [33]. Mineral carbonation otherwise called "mineral sequestration" includes a procedure where CO_2 from a capture step is carried into contact with a metal oxide-bearing material that contains alkaline earth metals, (e.g. calcium and magnesium) with the aim of fixing the CO_2 as insoluble carbonates [34].

The copying of weathering procedures (mineral CO_2 sequestration) at an accelerated pace allows calcium or magnesium containing minerals the opportunity to bond with gaseous CO_2 and construct strong carbonates (Eq. 2):

$$(Mg,Ca)_xSi_yO_{x+2y+z}H_{2z} + xCO_2 \rightarrow x(Mg,Ca)CO_3 + ySiO_2 + zH_2O \qquad (2)$$

The most suitable feedstocks for mineral CO_2 sequestration from natural minerals are the alkaline earth metals containing calcium and magnesium which are widely available. These minerals include olivine, serpentine and wollastonite. Magnesium and calcium comprise ~2.0 and 2.1 mol% of the earth's crust, respectively [35]. Another option for feedstocks is calcium rich alkaline solid wastes from industry that can be used in particular applications for CO_2 sequestration.

Mineral carbonation can be carried out ex situ in a processing plant after the extraction from a mine or production of residues in industry. It can also be carried out in situ by infusing gaseous CO_2 into underground geological formation which are capable of binding CO_2. Moreover, in terms of process, mineral carbonation routes can be divided into two groups; direct or indirect carbonation. Direct carbonation of minerals takes place in a simple and a single step that is either gas-solid or gas-liquid-solid process [36]. Several process routes for industrial mineral CO_2 sequestration have been reported [37]. However, indirect carbonation occurs in a multiple step process where first Ca-Mg reactive compounds undergo conversion processes and then go into carbonation routes as demonstrated in Figure 8 [38].

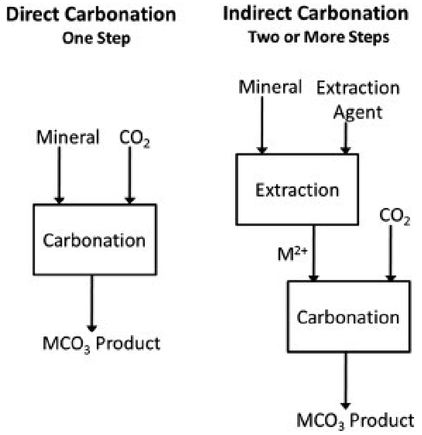

Figure 8 Direct and Indirect mineral carbonation, one step or two/more steps respectively. Note M refers to either calcium (Ca) or magnesium (Mg). [38]

2.4 Direct carbonation

Single step or direct carbonation has two main advantages over indirect carbonation techniques. Firstly, it does not require a complex experimental or industrial set up. Secondly, it requires minimal amount or variety of reagents. The direct carbonation method can occur in both gas-solid routes (dry environments) and in gas-liquid-solid process route (aqueous environments).

Direct carbonation with pre-treatment

Pre-treatment is usually undertaken to advance and quicken carbonation rates and efficiencies through raising the surface territory increment. The main procedures that have been developed include: chemical leaching, grinding, thermal and mechano-chemical pretreatments and are discussed below.

Direct carbonation with mechanical activation

Mechanical crushing and grinding are primarily performed to raise the surface area of the particles and reduce the particle size through dismantling and disarranging the mineral structure. Crushing is typically performed on dry materials, utilizing compression equipment such as jaw or cone crushers, whereas grinding is achieved by abrasion of the ore by the free movement of detached grinding media, such as rods, balls, or pebbles [39]. Turianicová et al. compares the reactivity of as-received and mechanically activated olivine in direct carbonation process to demonstrate that mechanically activated olivine has a higher affinity towards CO_2 sequestration than a non-activated sample [40]. Similar conclusions were drawn by Haug et al. and Fabian et al. who additionally demonstrated that high-energy attrition grinding of silicates results in higher conversion rates but consumes too much energy (as indicated in Table 1) [39,41].

Direct carbonation with thermal activation

Thermal activation of the hydrated Mg-silicate by the addition of a heat treatment stage in the mineral pretreatment process was studied by O’connor et al. [42]. The decomposition of Mg-silicate is shown below (Eq. 3).

$$Mg_3Si_2O_5(OH)_4 \rightarrow (MgO)_3(SiO_2)_2 + 2H_2O \quad (3)$$

They concluded that the most effective heat-treatment temperature was approximately 630°C observed in the TGA plot, which shows the most significant weight loss, due to dehydroxylation or removal of the chemically-bound water, was initiated at about 600°C. The theoretical energy required for the heat activation process is the sum of the enthalpy of dihydroxylation together with the energy spent increasing the mineral to 630 °C. As shown in Table 1, the electrical power needed for these reactions is 293 and326 kWh per t for antigorite and lizardite, respectively [42]. A study by Sanna et al. expanded this research to reveal that the energy requirement for 30 min pre-treatment at 610 °C could be lowered to 245 kWh per t instead of 326 kW h per t than previously reported (630 °C for 2 h) and thus contribute to an increased consecutive dissolution of serpentine from 60% to 90% in 5 minutes [43].

Table 1 Energy consumption for mechanical and thermal mineral feedstock pre-treatments [39,41,42,44,45].

Mechanical activation (olivine)	**RPM**	**Time (min)**	**SA (m^2g^{-1})**	**Crystalline Phase (%)**	**Energy Consumption (kW h per t)**
As- received	-	-	0.25	100	-
	1500	10	7.3	45	190
Attritor		30	18.1	26	580
		120	35.2	12	2310
Planetary	450	10	4.8	37	2010
		30	5.2	17	6030
Nutating	900	10	3	57	640
Attritor	1500	10	7.3	n.a.	170
Attritor	1500	30	18.1	n.a.	520
Attritor	1500	120	35.2	n.a.	280
Thermal activation (serpentine)			**Carbonation efficiency (%)**		**Energy Consumption (kW h per t)**
Antigorite (75µm)			62		293 (306)
Antigorite (38 µm)			92		293 (376)
Lizardite (75 µm)			9		326 (339)
Lizardite (38µm)			40		326(409)

Gas-solid process

The gas-solid route (dry route) allows for the carbonation minerals containing metal oxides to directly react with gaseous CO_2. Since it is the simplest method of carbonation, the only potential drawback of this technique is its slow reaction rate for large scale applications. However, the process can be potentially extremely energy efficient if feedstock is pre-treated, and pressure and heat are employed strategically. Since chemical balances favor gaseous CO_2 over strong bound CO_2 it is essential that the temperatures are controlled below the thermodynamic breaking points that occur at high temperatures [33], where the upper limit of the temperature for the mineral carbonation are dependent on the mineral type and the CO_2 partial pressure.

The gas-solid approach was the first to be studied because of its design simplicity [33] where a 30% serpentine conversion efficiency was reported at 300°C, 340bar [46]. However, even under such high temperature and pressure, the processes lasted for several days [46]. Some of these maximum temperature and pressure values for carbonation of several minerals are given in Table 2.

Table 2 Maximum carbonation temperatures at corresponding pressure for several minerals [33]

Mineral	**Tmax [°C]**	**p CO_2 [bar]**
Calcium oxide	888	1
Calcium oxide	1397	200
Magnesium oxide	407	1
Magnesium oxide	657	200
Calcium hydroxide	888	1
Magnesium Hydroxide	407	1
Wollastonite	281	1
Olivine	242	1
Serpentine	407	1

The kinetics of gas-solid carbonation

The kinetics of direct gas-solid carbonation of Air Pollution Control (APC) residues has been investigated by Baciocchi et al. under a thermogravimetric framework (TGA). They discovered that the kinetics were portrayed by a quick chemically-controlled reaction, proceeded by a slower product layer diffusion-controlled process. Carbonation rates were around 60 and 80 %, contingent upon the conditions of temperature, where temperatures close to or exceeding 400°C had no impact on the maximum carbonation, while CO_2 concentration had limited impact. The maximum carbonation rate was accomplished in 1 minute at 400°C and 50 vol% of CO_2 concentration [47]. The study recommended the utilization of 10 vol%, which had quick response rates and high carbonation rates in 3 minutes, and could bring down the expenses of capturing CO_2. Figure 9 shows these comparisons of carbonation rates of the first 5 minutes and shows that the rates are not sustainably different from each other.

The utilization of a self-structured and created fluidized bed gas-solid reactor with fly ash was employed by Reddy et al. [48]. They exposed the fly ash to flowing flue gas with the parameters given in Table 3.

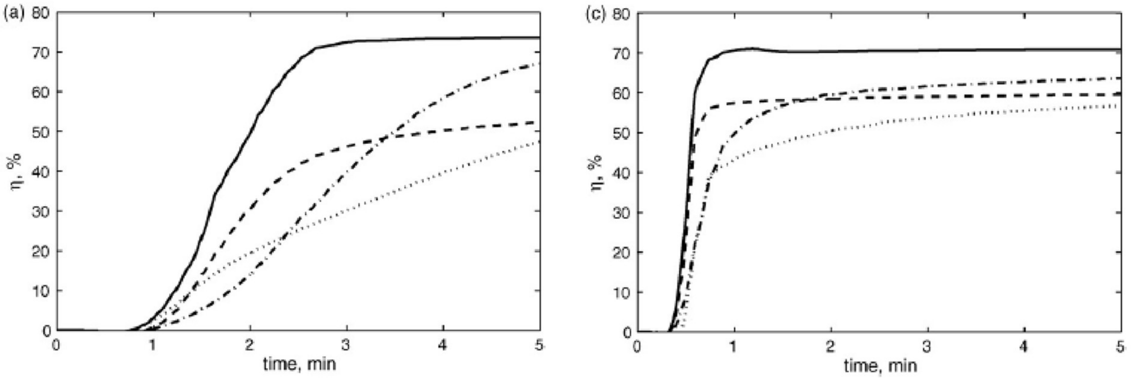

Figure 9 Calcium conversion vs. time in the first 5 min: (a) 10 vol.% of CO_2; (c) 50 vol.% of CO_2 at different temperatures: 350 °C (- - -); 400 °C (—); 450 °C (· · ·); 500 °C (-··-·-)[48].

Table 3 Summary of the experiment conditions

Expt. no.	Reactor temperature (K)	Humidifier temperature (K)	Ash quantity (kg)	Reactor pressure (Pa)	Gas flow Rate (m^3/s) (STP)
1	321-330	312-328	300	115,142.45	0.094
2	305-331	300-331	200	115,142.45	0.094
3	308-314	313	100	115,142.45	0.094
4	315-320	318	200	115,142.25	0.094

The calculated CO_2 carbonation cumulative averages and the carbonate content of the fly ash samples indicated that the maximum carbonation was observed at 10 minutes following which a slight drop in carbonation could be seen. The experiments further reflected the fact that CO_2 capture capacity of the amount of ash in the reactor was not fully exhausted after 1.5-2 hours of reaction. Additionally, the $CaCO_3$ content of flue gas treated fly ash samples ranged between 2.5 and 4% within 10 minutes of reaction. The maximum $CaCO_3$ content of fly ash was about 5.7% after about 1 hour of reaction. The total S and Hg contents of fly ash increased from virtually undetectable stages to 0.45 and 0.50

mg/kg, respectively. These results suggest that flue gas and Hg were also captured and mineralized by the fly ash particles.

Bhatia and Perlmutter studied these reaction rates and demonstrated that the rate is minimally affected when the partial pressure of CO_2 is considerably below the decomposition pressure levels [49]. Their study further revealed that a commencement period trailed by a growth section followed by a levelling off could be seen in the carbonation process. The reaction rate was sensitive to the temperature changes and escalated as the temperature was decreased. For 90 and 120 μm particle so over 70% of carbonation degrees could be achieved within a 1-minute period. After considerable carbonation occurred, mass transfer effects were also detected.

Nikulshina et al additionally performed a thermogravimetric analysis as a part of a three step thermochemical cycle to capture CO_2 where carbonation of CaO and $Ca(OH)_2$ was undertaken with 500 ppm CO_2 in the air at a controlled temperature of 200–450 °C [50]. They determined that the rate of CaO-carbonation was at the beginning chemically-controlled but goes through a transition to a diffusion-controlled system. They contended that this behavior of $Ca(OH)_2$-carbonation could be explained sufficiently by a kinetic model that acknowledges the formation of an interface of water molecules or OH-ions, and the underlying chemical reaction occurring over the surface that is not concealed by $CaCO_3$. The study conclusively showed that water catalyzes the CaO-carbonation to such a degree that, the reaction proceeds to 50% extent at a rate that is about 22 times quicker in the first 20 min, and the reaction extent reaches up to 80% at 400 °C after 100 min. These findings are also in accordance with the Avrami rate law (Eq. 4) that accurately models the CO_2 uptake by CaO or $Ca(OH)_2$ for heterogeneous chemical reactions [51,52]:

$$XCO_2 = \exp\,(-kt)^{\,n} \qquad (4)$$

where k and n are empirical parameters.

Mess et al studies the carbonation over significant time intervals of 15–20 μm particles of CaO at temperatures around the range of 550 and 1100 °C to show that after a fast reaction between 0.035 in under a minute, the rate impeded considerably [53]. At the beginning crystalline grains were spherical and around 1 μm across, however they developed after some time to the rough measurement of the particle. The moderate rate time frame was deciphered as a parallel diffusion process, with CO_2 diffusing at the same time down the grain limits and through the crystals produced. Intergranular splitting along the grain limits was noticeable in the highly carbonated samples.

Van Balen, K. studied the carbonation reaction of $Ca(OH)_2$ in ambient temperature of approximately 20 °C with different types of lime and the various CO_2 concentrations to identify the influence of different variables on the reaction kinetics. The data indicated that the carbonation reaction is zeroth order with respect to carbon dioxide concentration in the range (15–50%) at these temperatures. He asserted that the controlling factor in the carbonation process may be the dissolution of lime at the water-adsorbed surface. The highest reaction rate was proportional to the specific surface area of the lime when other variables are kept steady [54].

Koga, N. and Kodani, S. also studied reaction mechanisms of CO_2 capture by $Ca(OH)_2$ and CaO focusing on the kinetic modeling of the carbonation of $Ca(OH)_2$ as a consecutive reaction in a solid–gas system. They indicated that from physico-geometric consideration, the counter diffusion of water vapor and CO_2 through the surface product layer of $CaCO_3$ is necessary for the advancement of the overall $Ca(OH)_2$ carbonation process [55]. It was assumed that there is a layer of intermediate product (CaO) at the reaction interface zone between the internal $Ca(OH)_2$ and the external $CaCO_3$ in each reacting particle (see Figure 10). It was determined that the overall carbonation process consists of three partially overlapping reaction steps (N= 3), comprising two thermal decomposition steps and one carbonation step.

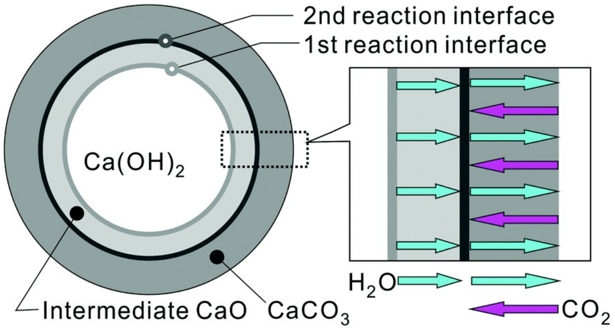

Figure 10 Expected reaction geometry and gaseous diffusion scheme for the reaction of $Ca(OH)_2$ with CO_2 [55]

Gas-liquid-solid process

In the gas-liquid-solid process route (aqueous route) CO_2 dissolves into the water forming HCO_3^-, where the dissolution amounts of CO_2 in the water change according to temperature and pressure [56]. In this technique Ca^{2+}/Mg^{2+} also leaches from the mineral structure and react with HCO_3^- to form Ca/Mg carbonates that precipitates in aqueous solution (Eqs. 5-7).

$CO_2 (g) + H_2O (l) \rightarrow H_2CO_3 (aq) \rightarrow H^+ (aq) + HCO_3^-(aq)$ (5)

$Ca/Mg\text{-silicate} (s) + 2 H^+ (aq) \rightarrow (Ca/Mg)_2^+ (aq) + SiO_2 (s) + H_2O (l)$ (6)

$(Ca/Mg)_2^+ (aq) + HCO_3^- (aq) \rightarrow (Ca/Mg)CO_3 (s) + H^+ (aq)$ (7)

The equilibrium constant of the reaction at 25°C is 1.7 x 10^{-3} meaning that CO_2 has low solubility in water, and thus largely remain as CO_2 molecules. As a consequence, the pH of the solution is only marginally affected by the reaction. Figure 11 further reflects how the dissolution of CO_2 into water varies depending on temperature and pressure [56].

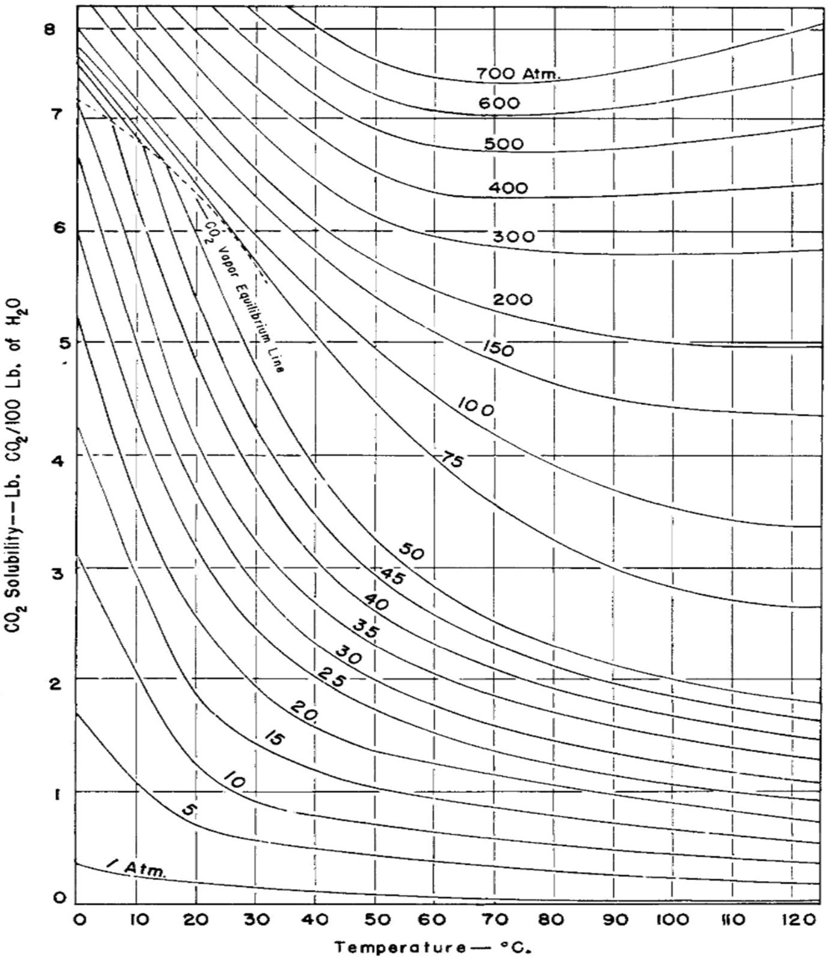

Figure 11 Dissolution degrees of CO_2 according to temperature and pressure [56]

2.5 Indirect carbonation

Indirect carbonation involves multi-step processes in order to achieve the desired outcome. These processes can be summarized mainly as extraction of metal ions from mineral structure, conversion to metal hydroxides and finally carbonation with gaseous or aqueous CO_2. In order to increase efficiency different routes have been tried throughout the research on indirect carbonation. Some of these procedures will be described shortly in the following sections as examples of indirect carbonation.

NaOH-based extraction

One of these processes includes NaOH as an extractive agent for metals to be separated from their structure. This route which include process parameters 200°C, p<15bar for 1-3 days has been developed by Blencoe et al. [57]. The feedstock mineral that has Ca in it reacts to form sodium calcium hydrosilicate in a solution of NaOH, in the meantime NaOH also reacts with CO_2 to produce Na_2CO_3. Lastly, the two products of the earlier reactions together with H_2O produce NaOH to be re-used and $CaCO_3$ and $NaCa_2Si_3O_8(OH)$ to be disposed.

Simplified version of overall reactions can be represented as following (Eq. 8):

$$3CaAl_2Si_2O_8\,(s) + 2\,CO_2\,(g) + 8\,NaOH\,(aq) \rightarrow CaCO_3\downarrow\,(s) + Na_8(AlSiO_4)_6CO_3\cdot 2H_2O\downarrow + 2\,Ca(OH)_2\,(s) \quad (8)$$

HCl extraction

This process uses HCl which is a strong acid to extract metals from silicate minerals in ambient pressure. First, HCl separates metal from mineral structure at 100°C and later at 150°C HCl is regenerated and with the reintroduction of water, these reactions thus produce metal hydroxides. Subsequently metal hydroxides are carbonated by gaseous CO_2.

Bioleaching

Bioleaching is an alternative route for extracting metals from natural or waste materials by using specific bacteria that alters mineralogy and extracts metals. It can also be used as a pre-treatment technique for carbonation. The potential of several bacteria (Bacillus circulans, Bacillus licheniformis, Bacillus mucilaginosus, Sporosarcinaureae) that have bioleaching properties towards the alteration of chemical and mineralogical properties of natural minerals (wollastonite and olivine) and alkaline waste residues (AOD and BOF steel slags, and MSWI boiler fly ash) is known [58]. Some known bacteria can convert the added acid generating substances (e.g. sulfides and elemental sulfur) into sulfuric acid as a side product of their biological process. Consequently, the sulfuric acid leaches out metal ions from the natural ore or industrial residues and the metals ions can then be carbonated for the purpose of CO_2 sequestration.

Ammonium salts extraction

Different ammonium salts have been investigated for multi-step mineralization processes. Serpentine and ammonium hydrogen sulphate were employed to produce an intermediate product (magnesium sulfate) which was then reacted with ammonium bisulphate for the precipitation of magnesium carbonate. An analogue process was developed by Wang and Maroto-Valer that aimed to extract magnesium from mineral rocks to produce different streams of useful by-products at ambient pressure [59]. The overall process created a closed loop thus avoiding the use of new additives, and allowing for the recovery and reuse of materials. However, the monetary evaluation of such a project remains speculative as a comprehensive economic evaluation of this procedure has not been completed yet. The generation of these items would help in lessening production costs as they may hold value in the market. On the other hand, utilizing ammonia and ammonium salts, which are destructive, includes utilizing appropriate materials for the reactors and channeling frameworks, expanding the expense of the innovation.

2.5 Points of interests and drawbacks in mineral carbonation

There are three prime advantages of CO_2 sequestration by mineral carbonation compared to other CO_2 storage methods.

Firstly, the process of carbonation is exothermic as established above. The carbonation reaction can be shown by the simple reaction of binary oxides, MgO and CaO (Eqs 9, 10). [60]

$CaO + CO_2 \rightleftharpoons CaCO_3 + 179$ kJ/mole [60] (9)

$MgO + CO_2 \rightleftharpoons MgCO_3 + 118$ kJ/mole [60] (10)

These reactions demonstrate that heat released through oxides and CO_2 interaction are greater in comparison to the heat released in the combustion of carbon (394kJ/mole). Additionally, the carbonation reactions of silicate structures also tend to be exothermic but with reduced levels of heat release. Consider for instance the carbonation reactions of forsterite and serpentine depicted below (Eqs 11, 12) [60] :

$\frac{1}{2}Mg_2SiO_4 + CO_2 \rightleftharpoons MgCO_3 + \frac{1}{2}SiO_2 + 95$kJ/mole [60] (11)

$1/3Mg_3Si_2O_5(OH)_4 + CO_2 \rightleftharpoons MgCO_3 + 2/3SiO_2 + 2/3H_2O + 64$kJ/mole [60] (12)

Secondly, the abundance of raw materials such as the natural deposits of serpentinite, and olivine minerals are more than sufficient to store the anthropogenic CO_2 that has already been emitted and could be produced around the world. MgO content in peridotite and serpentinized peridotite rocks can be as high as 35 to 40 percent by weight. The abundance of magnesium rich minerals and the readiness by which magnesium silicates react to CO_2 thus make the use of magnesium silicates suitable for above ground carbonation [61].

Thirdly, mineral sequestration is one of the stable and permanent form of carbon storage option currently available in the world. The finished products of mineral carbonates are environmentally safe and thermodynamically stable for over millions of years. In contrast to the other existing (or proposed) sequestration options (terrestrial, geological and oceanic) that can potentially leak with the passage of time and thus render CO_2 sequestration ineffective.

However, regardless of the points of interest recorded above, mineral carbonation experiences a range of scientific and monetary obstructions for further advancement and expansive scale exhibition. To start with, it is energy intensive process to prepare the natural mineral sources for carbonation process which includes mining, grinding, transportation. Furthermore, the speed of the chemical reaction rates which tends to slow down is a limiting factor for most carbonation routes together with particle interaction limitations regarding occurrence of $CaCO_3$ layers on the surface of the particle which limits the CO_2 diffusion. Other rate limiting factors can include structure of the mineral matrix which can affect also the dissolution. In general, interparticle and intraparticle porosities, specific surface area (SSA), particle size, partial pressure of CO_2 and CO_2 concentration are some of the main parameters that play crucial role in the carbonation ability of the minerals and kinetics of carbonation reactions.

2.6 Environmental considerations for mineral carbonation

Mineral carbonation processes, particularly whenever implemented on an industrial scale, may exhibit a few environmental problems. Firsts of all, if natural minerals are utilized as feedstock for carbonation, it would require large scale mining and processing operations. This would consequently influence the regular habitat/ecosystem and expand the contamination that results from the transportation of the material. Moreover, the clearance or utilization of the products must be considered. In the case of natural minerals, even if the product will be returned to mines as filling material, the storage capacity will not be enough as the product will have 1.5-2 times greater volume after processing. In case of reused industrial waste, the effect to nature and human health should be considered. If the industrial waste is not re-used, appropriate areas for their transfer and disposal need to be demarcated and allocated. Finally, the chemicals that are used as a reagent in the multi-step processes of indirect carbonation needs to be assessed and recycling or recovery of the chemicals needs to be assured (since reproducing these increases existing energy demands).

2.7 Carbonation of natural minerals (Ca/Mg-silicates)

In mineral carbonation the main challenge is to perform carbonation process an efficient and economically viable manner. Different application techniques have been tried to accelerate the carbonation of Ca and Mg containing minerals. One of the simplest methods is dry gas-solid direct carbonation [46]. In this process particles containing metal-oxides directly react with gaseous CO_2 at various temperature and pressures, where elevated temperature and pressure levels seems to be advantageous for the rate of the reaction. The greatest temperature at which the carbonation happens immediately relies upon the CO_2 partial pressure and the kind of mineral that is used.

An exergy investigation of direct dry carbonation of Mg-silicates has demonstrated that this procedure can result in a net exothermic heat impact [62]. Nevertheless, study shows that the rate of direct mineral carbonation is the most pressing issue to be emphasized. Actuation of the feedstock by heat treatment can altogether improve the reaction rate, however it is very energy intensive [63]. Since then, different methodologies have been investigated apart from direct gas-solid carbonation. Multi-step gas-solid carbonation options have been analyzed, [64] however slow reaction rates and thermodynamic limitations suggested that it is not feasible for the industrial application at the moment.

More research has been encouraged on direct or indirect aqueous carbonation of natural minerals but at the moment it is not applied on the industrial scale since it is not an economically viable option.

2.8 Carbonation of industrial residues and by products

As an alternative to natural minerals, idea of using industrial wastes as a feedstock for CO_2 mineralization have been researched [65]. Since the industrial residues tend to be chemically more unstable and more active compared to natural minerals, they do not require too much pre-treatment and the energy intensity of the process lower. Direct carbonation methods involving gas-solid or gas-liquid-solid processes are more attractive because of the diversity of elements that are present in waste which would affect the recovery of solvent. Also, the environmental considerations suggest that the product of direct carbonation process would be better for environment because the solid matrix that can retain contaminants is not demolished in the process and thus does not contribute to the leaching of heavy metals.

Ashes from combustion processes

The fossil fuel-power industry produces a lot of ash during the coal and OS conversion by thermal power plants. Bottom ash and fly ashes from electrostatic precipitators are produced in these power plants. Fly ash often contains a mixed and varied composition resulting from differences in the type and rank of coal (or the type and process of OS burned) where free CaO content ranges between 1wt% in bituminous coals and up to 30 wt% in BOS [65,66].

Incinerator Sewage Sludge Ash (ISSA) also emerges from combustion of sludge leftover and produces a silty-sandy textured sludge ash rich in CaO and MgO content (30wt% and 3wt% respectively) [67].

The residues of biomass and wood ash also act as good raw materials for direct carbonation and sequestration. These residues are produced through combustion, and usually contain powdery granulated amorphous particles, where the free CaO content varies in relation to the nature of biomass and wood burned and ranges from 24-46wt%. [68].

Construction sector waste streams

Ash is also abundantly produced in the cement industry which has cement kiln dust (CKD), cement by-pass dust (CBPD), ordinary Portland cement (OPC), recycled concrete aggregate (RCA) etc.

Although recycled concrete aggregate (RCA) is the main waste stream of this category, Cement kiln dusts (CKD) and cement by-pass dust (CBPD) also have great carbonation potential because of their free lime content. Obtained from demolition operations, RCA`s quality depends on the separation process the RCA undergoes. Typical free CaO content of samples from UK is usually 17wt% [69].

Cement kiln dusts (CKD) and cement by-pass dust (CBPD) are fine by-products of portland cement and lime high- temperature rotary kiln production operations. CKDs are captured in the air pollution control dust collection system. Ca content in this waste stream can usually be as high as 35.50wt% [70], however, since it does not have high content free CaO, it is not suitable for carbonation. CBPD on the other hand is rich in Ca which is found as free CaO and portlandite, it is a suitable candidate for mineral carbonation.

Metal waste streams

Metal waste streams are also considered to have potential for as CO_2 sorbents. Some of these metal industry wastes are Air- or Water-Cooled Copper Slag (CS), Phosphorus slag (PS), Ground granulated blast furnace slag (GGBS), Steel slag (SS). Each of these slags has slightly different characteristics. When the high temperature slag is cooled slowly in air, it forms a dense, hard crystalline product while pouring molten slag into water produces a granulated amorphous slag with slightly less calcium and magnesium oxides present [71]. CaO and MgO content in copper smelt slag have been reported in the range 0.6-10.9wt% and 0.75-3.7wt% respectively [72]. Phosphorus slag tends to be black to dark gray, vitreous (glassy), and of irregular shape with a CaO content of around 44wt% [73]. Ground granulated blast furnace slag (GGBS) is a by-product obtained from production of pig iron in blast furnaces and produces glassy aggregate granules rich in roughly 33wt% [74]. Steel slag (SS) is the by-product obtained from the manufacturing process of steel from pig-iron with typical CaO values between 41-42wt% [75].

Other materials

Alternative minor waste products including red sludge, air pollution control residues and paper sludge also contain appropriate chemical compositions for mineral carbonation. Red sludge is a waste slurry, mainly composed of iron oxide, produced from the generation of alumina from bauxite. It is estimated that the yearly global generation of red slurry is around 77 million tons [76]. Red mud chemical composition may include Al2O3 (10-20wt%) and free lime (2-8wt%) [77].

Air pollution control wastes, which are obtained by trapping particles that are harmful to environment from gaseous emissions during burning of wastes at incineration plants generally, contain free lime content between 50-60wt% [47]. Lastly, paper sludge incinerator ash which is produced from incineration of the waste residue of the paper production process also contains a free lime content can between 40-65wt% [78].

2.9 Aim and scope

It can be seen from arguments in literature review that there is a huge concern over the impact of increasing concentrations of GHG, primarily CO_2, which is emitted by growing power and cement industries. Mineral carbonation by industrial waste is a prominent option of CCS for countries with no geological storage option, such as Estonia. In addition to this, stabilization of waste material and possible valorization of these materials by carbonation is critical for protection of the environment and transitions towards a circular economy. As indicated in the literature review, although mineral carbonation studies of different waste materials with different process routes have been conducted around the world, there is a limited work related to direct gas-solid carbonation of BOS and BPD that analyzes the effects of pretreatment and temperature on capture capacities and capabilities.

The aim of this master thesis is to obtain both experimental and operational knowledge by studying thermal characteristics of CO_2 mineralization, reaction mechanisms and kinetics of selected industrial residues (BOS and BPD) by investigating the effects of pre-treatment (hydration and grinding) at different process temperatures. The following specific objectives were the main subjects investigated in this thesis study:

- Detailed chemical, physical and thermal characterization of the selected samples including SSA, PSD, XRD, TGA for pre-evaluation of carbonation potentials.
- Comparison of CO_2 uptake capacities of BOS and BPD samples under 100 % CO_2 at different temperatures.
- Comparison of CO_2 uptake thermograms of carbonation processes of BOS and BPD samples obtained from thermal analysis with TGA.

- Effect of activation by hydration and grinding on reactivity and CO_2 uptake capacity at different temperatures.
- Applicability of the carbonation process in bigger dimensions by using rotating tube-furnace to obtain preliminary operational knowledge and demonstration.

3. MATERIALS AND METHODS

3.1 Industrial residue samples

Three different types of waste residues from OS and cement industry were chosen and named as BOS1 represents burnt OS samples from total ash silo of circulating fluidized bed (CFB) boilers of Balti power plant (PP) in Estonia and BOS2 represents burnt OS samples from the electrostatic precipitators (ESPA) of Auvere power plant also located in Estonia. Whereas, BPD represents the cement by-pass dust obtained from Robilante (Italy) cement factory as part of the project work. The sampling period for BOS samples was February 2018 and for BPD was September 2018.

3.2 Preparation and characterization of samples

The original (dry) and hydrated samples for each residue have been prepared. Hydrated samples have been prepared with liquid to solid ratio of 0.2 w/w in a semi-batch Eirich EL1 type intensive mixer shown in Figure 12 below. The samples were mixed with water at a rotation speed of 300 rpm for 20 minutes. Hydrated samples were later dried at 105°C for 4 hours. These samples have also been ground in a Retsch PM 100 grinding machine in a four-ball planetary mill as pretreatment incase the uptake level of CO_2 depending on SSA.

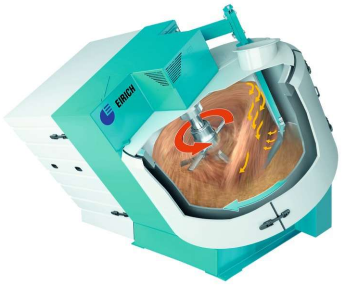

Figure 12 Eirich EL1 type intensive mixer

The materials were analyzed using XRF spectroscopy (Rigaku Primus II) and quantitative X-ray diffraction (XRD, Bruker D8 Advanced) at the Department of Geology, University of Tartu.

The contents of free lime (fCaO), by ethylene glycol method (Reispere 1966) and mineral CO_2 using Electra CS - 580 Carbon/Sulfur Determinator were determined. In addition, the Brunauer–Emmett–Teller (BET) SSA and the particle size distribution (PSD) were determined using a Kelvin 1042 sorptometer and Horiba laser scattering particle size distribution analyzer LA-950, respectively.

3.3 Experimental set-up

Gas–solid carbonation experiments under isothermal conditions

The SetaramSetsys Evo 1750 thermoanalyser was used to investigate the mass gain representing the CO_2 uptake during the carbonation of BOS1, BOS2 and BPD. During the experiments, standard 100 µLAl_2O_3 crucibles were used and 10±0.5 mg of the sample was weighted. The isothermal tests were performed at 4 different temperatures (300, 400, 450, 500°C) for hydrated samples and for original (non-hydrated) samples at 7 different temperatures (300, 400, 450, 475, 500, 550, 600°C) for 30 minutes. Hydrated samples were not tested at 550 and 600°C in order to eliminate the dihydroxylation of the $Ca(OH)_2$ particles which can occur in the temperature range of 500 and 600°C. Ground samples were also tested at 400, 500, 600°C. Overall temperatures higher than 600 °C have been avoided in order to increase the applicability of energy efficient process at somewhat lower temperatures compared to well-known carbonation temperature of CaL process (650-700°C) . All thermogravimetric (TG) tests were carried out in 100% CO_2 atmosphere by switching the inert atmosphere of 100%Ar when desired temperature is reached. The flow of CO_2 was kept constant at 50 mL min^{-1} across all experiments.

Gas–solid carbonation experiments under non-isothermal conditions

The non-isothermal tests were performed under the following conditions: sample mass of about 10±0.5 mg, standard 100 µL Al_2O_3 crucibles, heating rate of 10 K min^{-1}, temperature range from 30 (303K) to 1000°C (1273K) and 100% CO_2 and gas flow rate was set to 50mL min^{-1} for all experiments. Sample mass gain/loss and associated thermal effects were obtained by TGA/DTA curves. In order to identify the different mass gain/loss steps, the TGA first derivative (mass gain/loss rate) was also used.

Gas–solid carbonation experiments in rotating tube-furnace

Nabertherm rotating tube-furnace with parameters; T max of 1200 °C; Furnace tube diameter of 70-90 mm was operated for bigger scale gas solid carbonation of the samples in order to determine the applicability of the process to wider scale operations (see Figure 13). 200 g hydrated and non-hydrated samples were led into horizontal quartz tube furnace. The samples were heated in the atmosphere of 100% N_2 up to 400±10°C and then CO_2 gas was fed into the tube furnace for 30 minutes. Rotation speed was kept at 5 rpm in order to enable easier solid-gas contact and diffusion of CO_2. CO_2 entered the tube at the inlet with a rate of 100 L hr^{-1} during the isothermal process. After cooling the samples were taken for the mineral CO_2 and fCaO determination tests. The initial and carbonated samples were analyzed also with FTIR spectrometer ALPHA in order to compare mineralogical changes. FTIR measurements were recorded in the 400–4000 cm^{-1} region.

Figure 13 Nabertherm rotating tube-furnace

Physical characteristics

SSA changes due to hydration and grinding and particle size distribution and are characterized below.

Carbonation of lime was shown to very much depend on the SSA of the hydrated lime particles [45]. It is known that hydration of lime increases SSA of the particles [46]. From BET SSA tests we can see that the SSA of all the samples have increased after initial hydration (see Figure 14). Highest increase happened on BPD, initial sample had SSA of 3.84 m^2/g with mean particle size of 40.87 µm, after the hydration it rose to SSA of 7.02 m^2/g.

Before hydration the sample characterized with highest SSA was BOS2 with a mean particle size of 20.98 µm and SSA of 6.05 m^2/g, while SSA increased to 6.85 m^2/g after hydration. BOS1 with a mean particle size of 50.62 µm had SSA of 2.82 m^2/g which increased µm to 4.35 m^2/g after hydration. The particle size distribution is given on Figure 16. Grinding has increased the SSA of BOS1 and BPD while decreasing SSA of BOS2 (see Figure 15).

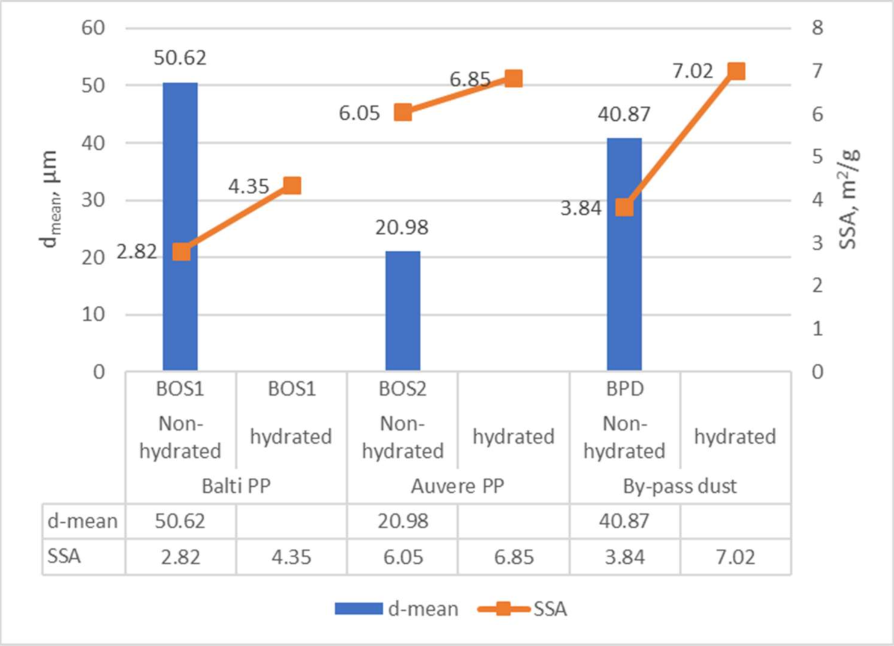

	BOS1 Non-hydrated	BOS1 hydrated	BOS2 Non-hydrated	hydrated	BPD Non-hydrated	hydrated
	Balti PP		Auvere PP		By-pass dust	
d-mean	50.62		20.98		40.87	
SSA	2.82	4.35	6.05	6.85	3.84	7.02

Figure 14 Mean particle size (d_{mean}) and BET SSA of the samples after hydration

SSA of the samples indicate that after hydration BPD have the highest increase which suggest more carbonation ability. In non-hydrated condition highest SSA belongs to BOS2 which means higher carbonation ability attributed to SSA for non-hydrated samples.

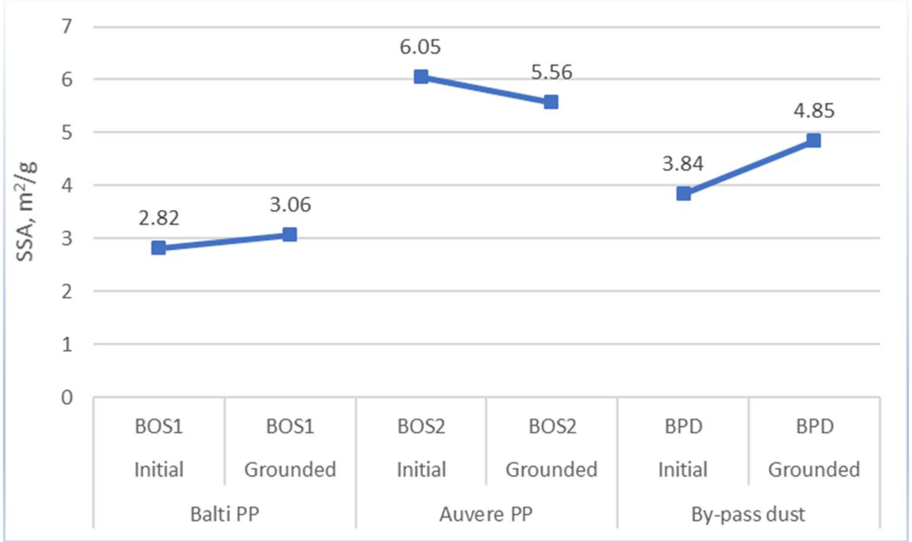

Figure 15 BET SSA of the samples after grinding

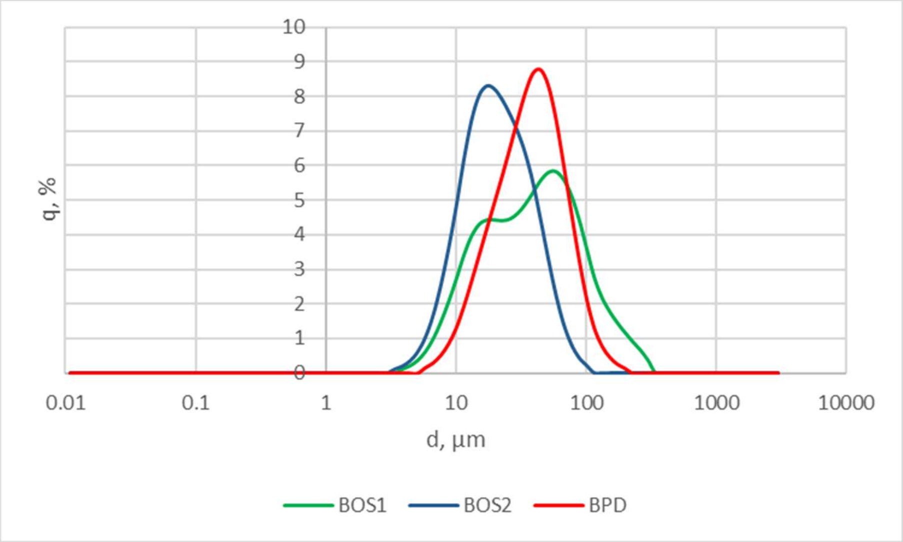

Figure 16 Particle size distribution of the samples.

Chemical and phase composition

According to XRF analysis, the BOS samples and the BDP composes of mainly Ca- and Si-compounds adding up 60-75%. The sample of BPD contains considerable amount of free lime (37.49%) and portlandite, total CaO content is 61.2% (see Figure 17). Additionally, it contains 17.2% C2S, 4.0% wollastonite and 4.0% merwinite that could also be considered as CO_2 binding minerals (see Figure 14). The content of quartz, calcite and anhydrite is 5.3%, 3.2% and 4.7%, respectively. The BOS samples also have reasonably good amounts of free lime (BOS1-12.6% and BOS2-18.5%). The phase composition indicates that both BOS samples and the BPD contains a considerable amount of lime, portlandite and secondary Ca-silicates as well (See Figure 18).

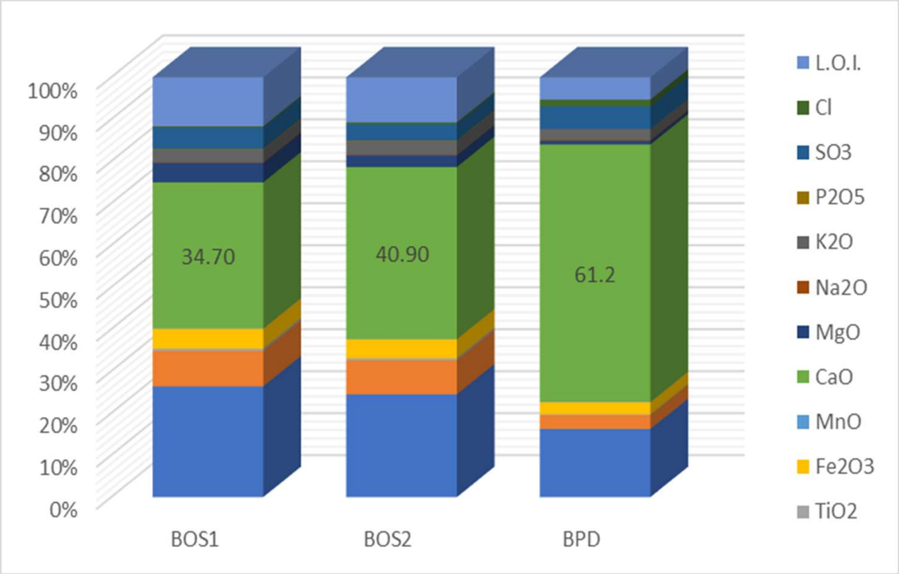

Figure 17 Chemical composition of the samples

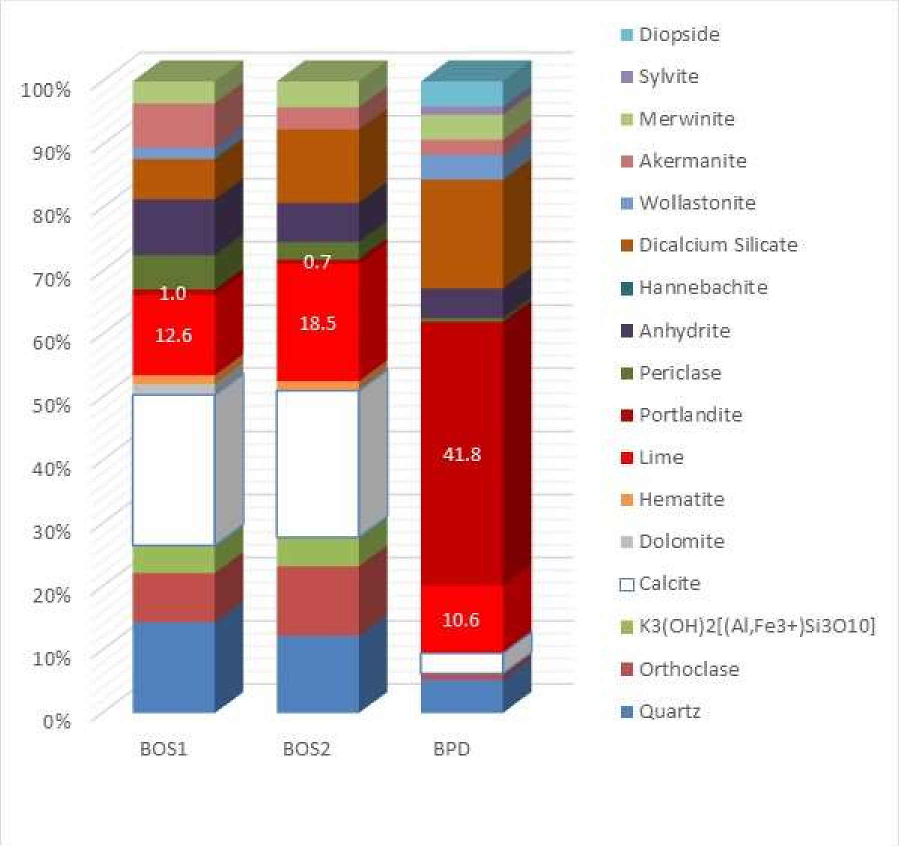

Figure 18 Phase composition of the samples

The quantitative XRD analysis indicated that samples contained considerable amount lime, portlandite and secondary Ca-silicates, which attribute as potential CO_2 binders (see Figure 18). In order to estimate and compare the CO_2 binding ability of different materials the CO_{2max}, the maximal possible CO_2 content of the sample, was calculated on the basis of CO_2, fCaO, $CaSiO_3$, Ca_2SiO_4 and $Ca_3Mg(SiO_4)_2$ content of initial sample as shown below (Eq. 13).

$$CO_{2\max} = \frac{\frac{fCaO \times M_{CO_2}}{M_{CaO}} + \frac{CaSiO_3 \times M_{CO_2}}{M_{CaSiO_3}} + \frac{2 \times Ca_2SiO_4 \times M_{CO_2}}{M_{Ca_2SiO_4}} + \frac{3 \times Ca_3Mg(SiO_4)_2 \times M_{CO_2}}{M_{Ca_3Mg(SiO_4)_2}} + CO_2}{100 + \frac{fCaO \times M_{CO_2}}{M_{CaO}} + \frac{CaSiO_3 \times M_{CO_2}}{M_{CaSiO_3}} + \frac{2 \times Ca_2SiO_4 \times M_{CO_2}}{M_{Ca_2SiO_4}} + \frac{3 \times Ca_3Mg(SiO_4)_2 \times M_{CO_2}}{M_{Ca_3Mg(SiO_4)_2}}} \times 100,\% \qquad (13)$$

Theoretical CO_2 binding potential of BPD sample which contains 37.49% of free lime as well as Ca-silicates as additional CO_2 binders seems very promising. The free lime content of BOS1 and BOS2 is 14.02% and 16.43% respectively (see Figure 19)

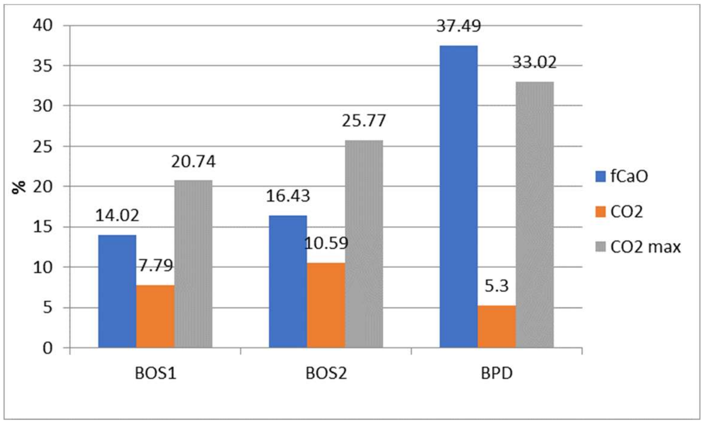

Figure 19 Mineral CO_2 and fCaO content of initial burnt oil shale (BOS) and cement bypass dust (BPD) samples

4. RESULTS AND DISCUSSION

4.1 Non-isothermal analysis

Figure 20 presents the comparisons of thermal decomposition profiles with TG-DTG curves (mass change (mg/10mg) vs. temperature °C) belonging to all hydrated and non-hydrated samples of BOS1, BOS2 and BPD under 100 % Ar with a heating rate of 10K min^{-1}. For the BPD samples three mass loss steps can be identified. First and the biggest fall can be observed both in TG and DTG curves in the temperature range of 360-460 °C which indicates the decomposition of $Ca(OH)_2$ shown below (Eq. 14).

$Ca(OH)_2 \rightleftharpoons CaO + H_2O$ (14)

Activated sample shows higher mass change due to the decomposition of $Ca(OH)_2$, which was expected due to hydration of free lime in the original sample. The second fall indicates the decomposition of dolomite and $CaCO_3$ which happens in the temperature range of 580-700 °C. After 700 °C calcium silicate minerals can also start to play role forming new crystal phases and make structural reorganization as a third step of mass loss which continues until 1000°C. For the BOS samples it is inferred that there are two distinct steps throughout decomposition for the hydrated and non-hydrated samples. Similar to BPD, the main first mass loss step is related to decomposition of $Ca(OH)_2$ in the same temperature range (360-460 °C).

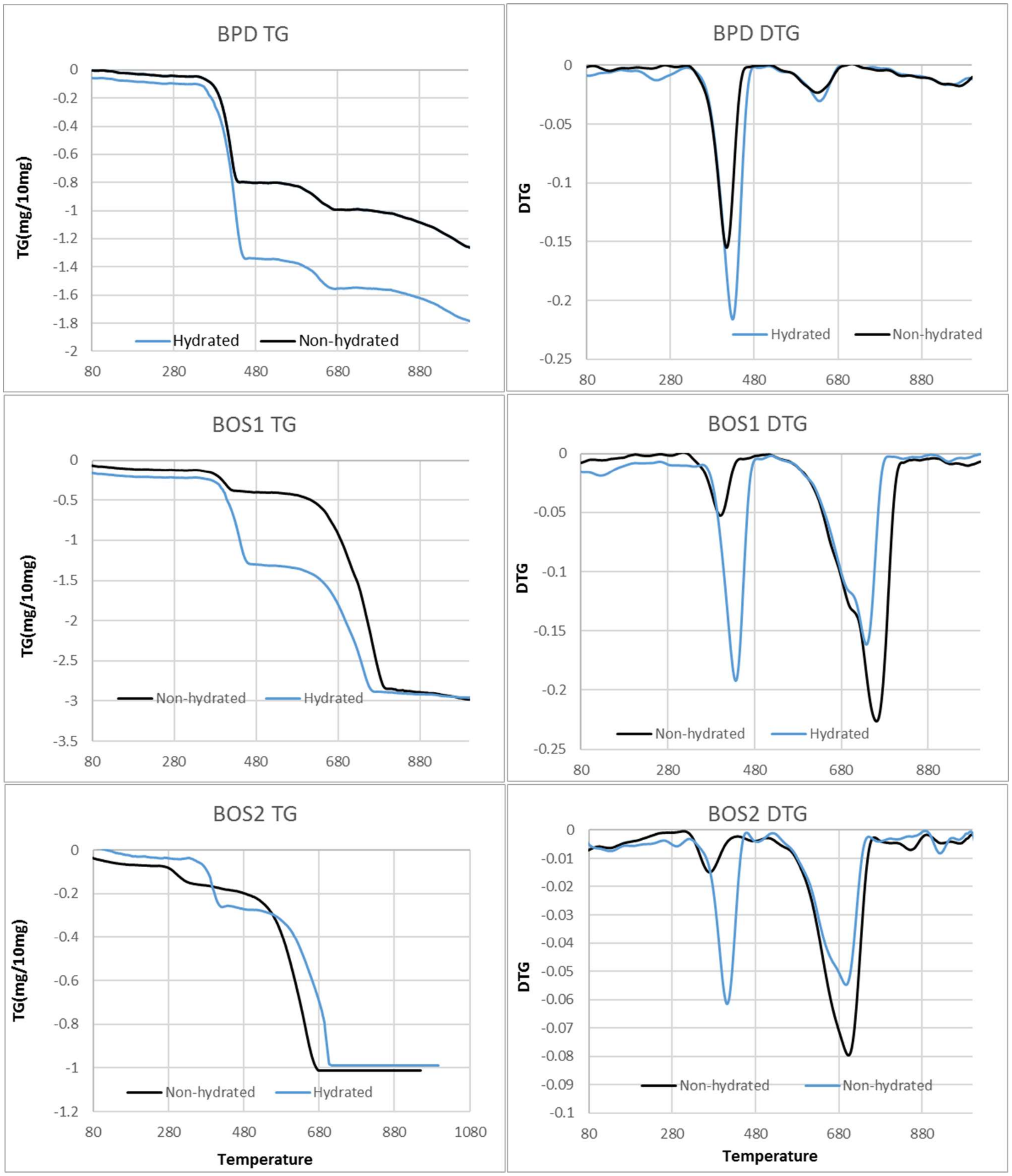

Figure 20 TG and DTG non-isothermal curves

4.2 Gas–solid carbonation under isothermal conditions

Thermal analysis of BOS1, BOS2, and BPD have been presented in Figure 21-a, 21-b and 21-c representing the CO_2 uptake (mgCO_2/10mg) curves under 100% CO_2 atmosphere. The curves that obtained at 300 °C have not been added as they have shown negligible amount of carbonation rates for the non-hydrated samples which are kept out for the comparison purposes. However, for hydrated samples isothermal data for 300 °C has been used for kinetic calculations.

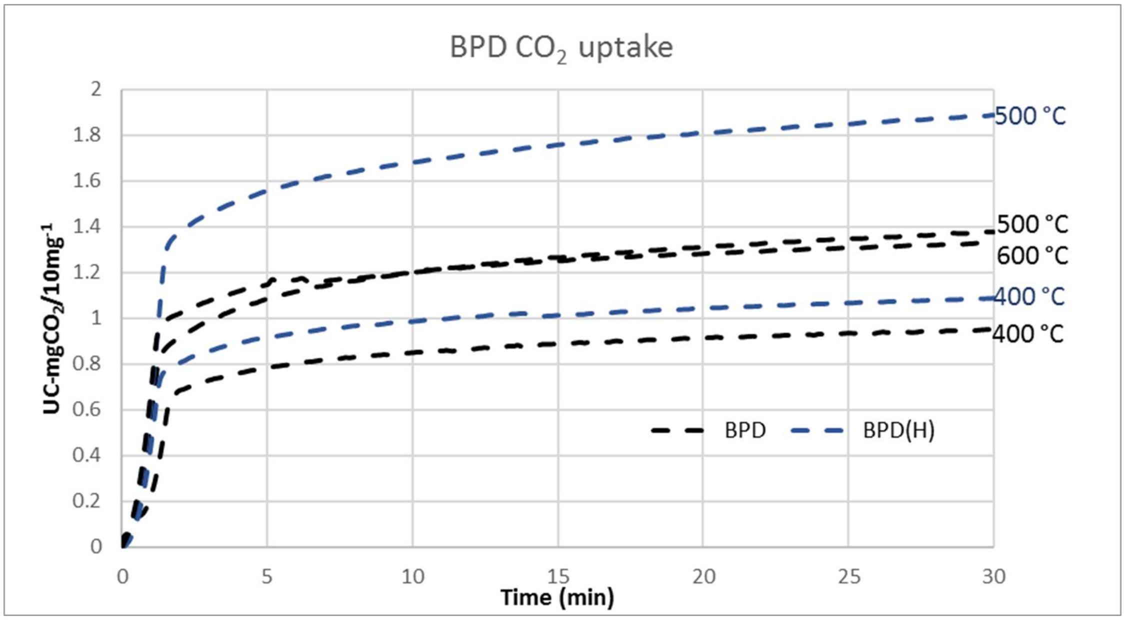

Figure 21-a BPD isothermal TG curves

Curves of non-hydrated BPD sample shows that at 500 and 600 °C the uptake capacity (UC) values are quite similar which can be interpreted that temperature increase does not change the UC at this interval (see Figure 21-a) without hydration. However, UC values of non-hydrated BOS1 and BOS2 samples increase at 600 °C compared to 500 °C. Results have shown that hydrated samples have gained the ability of higher CO_2 binding capacity for all the samples both at 400 and 500 °C. It is also visible that 80-90 % of the final UC has been reached in the first 2-3 minutes at 500 °C. The non-activated samples have an initial rate comparable to the hydrated samples, yet the reactivity tends to slow-down which results in lower UC values compared to hydrated samples in the same given limited of time. TG tests indicate that the carbonation process is quite fast at the first stage due to the large reaction surface available and after 2nd minute it slows down due to the decrease in surface area and increasing product layer diffusion resistance.

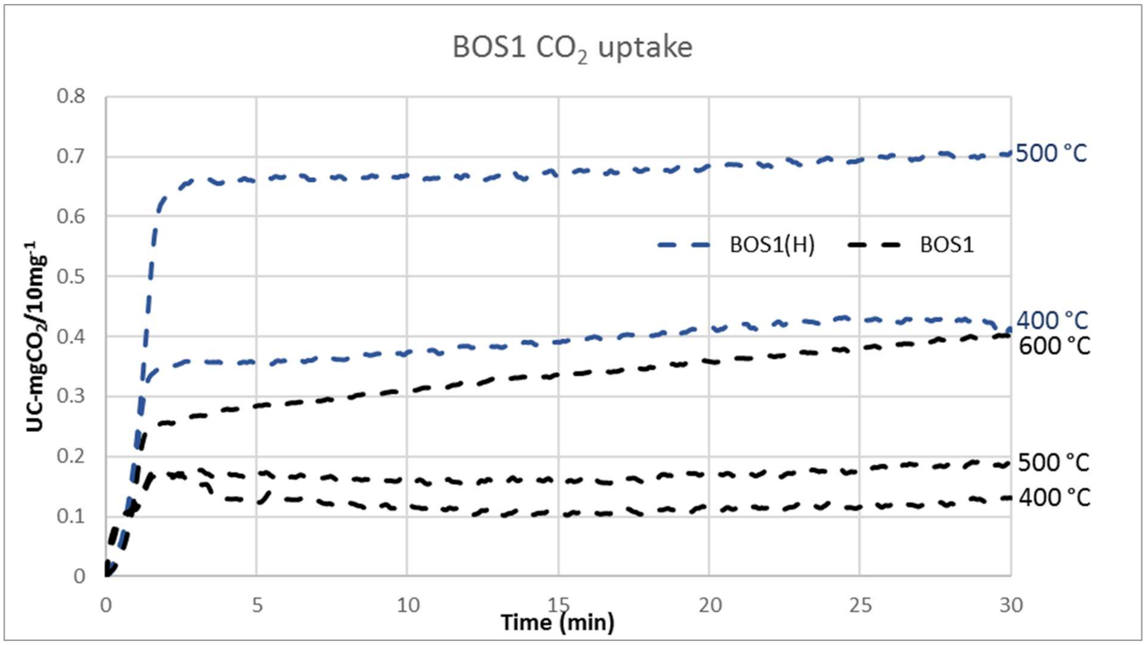

Figure 21-b BOS1 isothermal TG curves

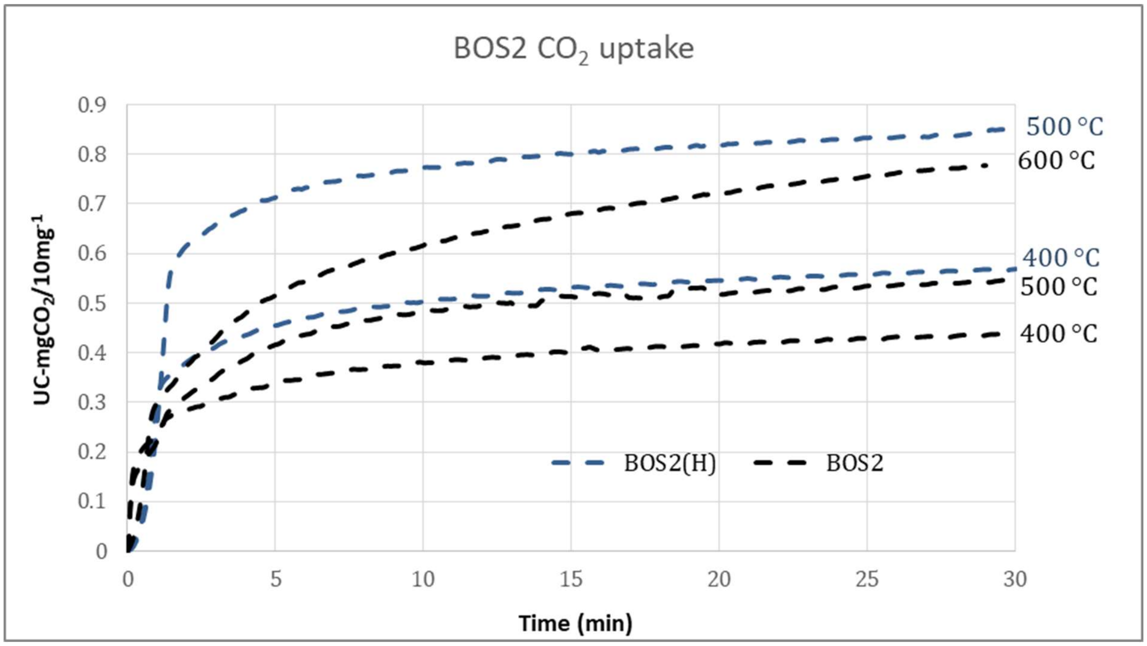

Figure 21-c BOS2 isothermal TG curves

The non-hydrated BOS1 sample has quite similar UC values at 400-500 °C, while hydrated BOS1 sample has substantial difference in UC values at same temperatures and has much higher UC values (see Figure 21-b).

Effect of mechanical treatment

Although the BET surface area of BOS1 was increased from 2.83 m^2/g to 3.06 m^2/g and similarly, BPD BET surface area was also increased 3.84 m^2/g to 4.85 m^2/g after grinding, the grounded samples that were tested at 400-500-600 °C showed an unexpected slight decrease in the reaction rates and their binding ability. For this reason, the TA curves for the grounded samples have not been reproduced here.

4.3 Kinetics of binding reactions

Calculations for the purpose of determining the reaction mechanism of the first fast stage of the carbonation reaction up to 2 min without including the second slow stage have been made based on the isothermal data and using different well-known reaction mechanisms presented on Table 4 [79] and the experimental data from isothermal curves at different temperatures were fitted to a set of kinetic models, according to the following equations.

Jander's three-dimensional diffusional (D3) model is one of them and based on the assumption of spherical solid particles of same size are embedded in continues medium [80]. This model uses unreacted core approach and tries to solve the shifting boundary diffusion problem due to the shrinking of the unreacted layer in a quasi-steady-state style [81]. The rate of a solid-state reaction can be generally described by (Eq. 15):

$$\frac{d\alpha}{dt} = Ae^{-(E_a/RT)}f(\alpha) \qquad (15)$$

where, A is the preexponential (frequency) factor, E_a is the activation energy, T is absolute temperature, R is the gas constant, $f(\alpha)$ is the reaction model, and α is the conversion fraction [81]. For a gravimetric measurement, α is defined by (Eq. 16):

$$\alpha = \frac{m_0 - m_1}{m_0} \qquad (16)$$

where, m_0 is initial weight, m_t is weight at time t, and m_∞ is final weight. Since weight = volume × density (ρ), the weight of n spherical particles is (Eq. 17):

$$weight = \frac{4}{3}n\rho\pi r^3 \qquad (17)$$

The conversion fraction for a reaction involving n spherical particles using eq 16 and 17 is :

$$\alpha = \frac{\frac{4}{3}n\rho\pi R^3 - \frac{4}{3}n\rho\pi(R-x)^3}{\frac{4}{3}n\rho\pi R^3} \qquad (18)$$

where *x* is the thickness of the reaction zone. Upon simplification, eq 18 becomes (Eq. 19)

$$x = R\left(1 - (1 - \alpha)^{1/3}\right) \qquad (19)$$

Jander used the parabolic law to define *x* [80]. Therefore, assuming *k* '= *k*/*R*^{2}, eq 19 becomes the D3 (Jander) model (Eq. 21):

$$(1 - (1 - \alpha)^{1/3})^2 = k't \qquad (20)$$

In order-based (F) models as a second model practiced, the reaction rate is proportional to concentration, amount or fraction remaining of reactant(s) raised to a particular power (integral or fractional) which is the reaction order [81]. Order-based models are derived from the following general equation (Eq. 21):

$$\frac{d\alpha}{dt} = k(1 - \alpha)^n \qquad (21)$$

By separating variables and integrating eq 21 the first-order model (F1) model is obtained when n = 1 (Eq. 22)

$$-\ln(1 - a) = kt \qquad (22)$$

The first-order model, also called the Mampel model [82], is a special case of the Avrami−Erofeyev (A) models where *n* = 1.

These solid-state kinetic models have been used to simplify the kinetic calculations of heterogeneous materials and to compare reaction rates of hydrated and non-hydrated samples that has been utilized in this work.

Table 4 Classification of Mathematical Expressions of Reaction Mechanisms [79]

Kinetic Classification		**$f(\alpha) = (d\alpha/dt)/k$**	**$g(\alpha) = \int d\alpha/f(\alpha) = kt$**
Based on diffusion mechanisms			
D1	Plane symmetry	$1/2\alpha$	α^2
D2	Cylindrical symmetry	$[-\ln(1-\alpha)]^{-1}$	$(1-\alpha)\ln(1-\alpha)+\alpha$
D3	Three-dimensional	$(3/2)\,(1-\alpha)^{2/3}[1-(1-\alpha)^{1/3}]^{-1}$	$[1-(1-\alpha)^{1/3}]^2$
D4	Spherical symmetry	$(3/2)\,[(1-\alpha)^{-1/3}-1]^{-1}$	$(1-2\alpha/3)-(1-\alpha)^{2/3}$
Based on geometrical models			
R1	Plane symmetry	1	α
R2	Cylindrical symmetry	$2(1-\alpha)^{1/2}$	$1-(1-\alpha)^{1/2}$
R3	Spherical symmetry	$3(1-\alpha)^{2/3}$	$1-(1-\alpha)^{1/3}$
Based on “order” of reaction			
F1	First-order	$1-\alpha$	$-\ln(1-\alpha)$
F2	Second-order	$(1-\alpha)^2$	$-1+(1-\alpha)^{-1}$
F3	Third-order	$(1-\alpha)^3$	$[-1+(1-\alpha)^{-2}]/2$
Based on nucleation and nucleus growing			
N1		$4\,(1-\alpha)\,[-\ln(1-\alpha)]^{3/4}$	$[-\ln(1-\alpha)]^{1/4}$
N2		$3\,(1-\alpha)\,[-\ln(1-\alpha)]^{2/3}$	$[-\ln(1-\alpha)]^{1/3}$

Well known general equation for solid-state reaction kinetics shown in equation (23):

$$f(\alpha) = (d\alpha/dt)/k \qquad (23)$$

where $f(\alpha)$ is certain function of a, t represents the time, α is the extent of the reaction or fraction converted, and k is the rate constant. By integration of equation (23) we get:

$$g(\alpha) = \int d\alpha/f(\alpha) = kt \qquad (24)$$

where $g(\alpha)$ is the integral form of the kinetic model, the graph of $g(\alpha)$ versus the reaction time is a straight line, whose slope is the rate constant, k. Following this, since the Arrhenius dependent to the rate constant with the temperature, the activation energy can be subsequently calculated by the graph of the logarithm of the rate constants versus the inverted temperature values (Eq. 25):

$$\ln(k) = lnA - \frac{E_a}{RT} \qquad (25)$$

The data is fitted to the kinetic models for each different hydrated and non-hydrated sample for three different temperatures. According to highest yield of regression factors (R^2) it is determined that for BOS2 sample overall carbonation process is controlled by CO_2 intraparticle three-dimensional diffusion mechanism (D3). Three-dimensional diffusion (D3): $[1 - (1 - \alpha)^{1/3}]^2 = kt$

According to the selected most appropriate mechanism functions (D3, A2) the kinetic parameters have been calculated and the relationship between 1/T and ln*k* for BOS2 and BPD can be seen in Figure 22. According to the slopes and intercepts of the fitting straight lines activation energy (E_a) and pre-exponential factor (A) values were obtained for all samples and shown in Table 1.

At all selected temperatures higher carbonation rates belong to the hydrated samples compared to non-hydrated samples. Although the rates are temperature sensitive, temperature rise is not as effective as hydration treatment even when the lowest and highest temperatures are compared in terms of the determined reaction rates. The hydration treatment is clearly more effective for BOS samples, especially, for BOS1; increasing the rates of carbonation reactions significantly at certain temperatures compared to non-hydrated cases. Due to the higher carbonation rates of hydrated BOS samples, the obtained E_a values are lower for hydrated samples, yet the hydration causes to increase of E_a value for the hydrated BPD.

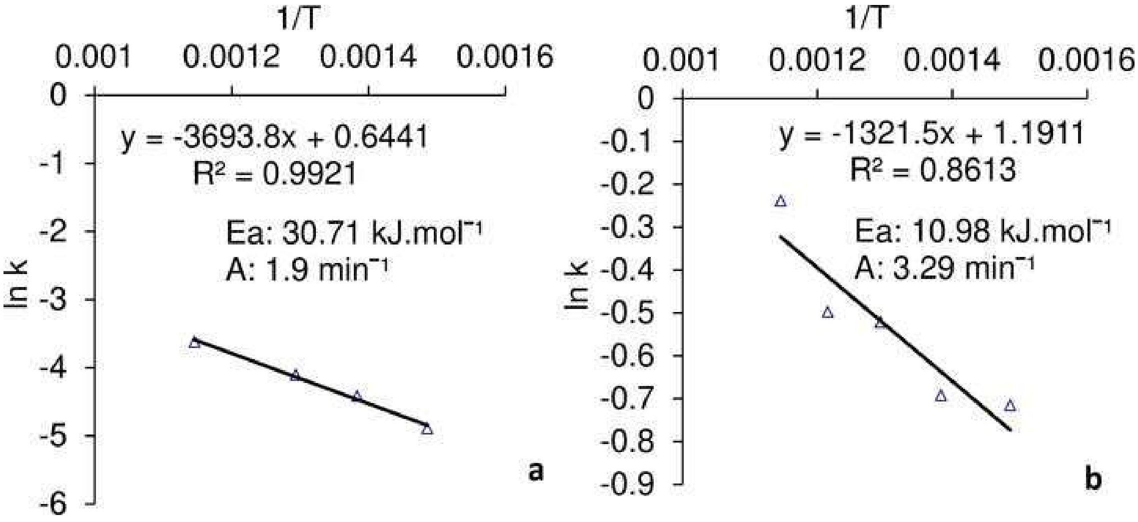

Figure 22 Arrhenius plots of BOS2(a) and BPD(b)

Table 5 k values for each temperature and linear correlation coefficient (R2) for the most reasonable mechanism function, obtained Ea and A values for all samples

Sample →	**BOS1**	**BOS1(H)**	**BOS2**	**BOS2(H)**	**BPD**	**BPD(H)**
Model →	*D3*	*A2*	*D3*	*A2*	*A2*	*A2*
T/K	***k*** / **R^2**	***k*** / **R^2**	***k*** / **R^2**	***k*** / **R^2**	***k*** / **R^2**	***k*** / **R^2**
573	-	-	-	-	-	*0.26* **0.822**
673	*0.0028* **0.9563**	0.49 **0.942**	*0.0075* **0.8288**	0.47 **0.8397**	*0.49* **0.8324**	*0.54* **0.9497**
723	*0.0032* **0.9783**	0.51 **0.9641**	*0.012* **0.9005**	0.5 **0.9769**	*0.5* **0.9837**	*0.74* **0.965**
748	-	0.54 **0.9545**	-	0.55 **0.9745**	-	*0.79* **0.9828**
773	*0.0046* **0.9576**	0.63 **0.9765**	*0.017* **0.9801**	0.68 **0.9677**	*0.59* **0.9604**	*0.97* **0.9416**
823	*0.0065* **0.7898**	-	-	-	*0.61* **0.9572**	-
873	*0.029* **0.7976**	-	*0.028* **0.9294**	-	*0.78* **0.9417**	-
E_a/ kj.mol^{-1}	**47.67**	**9.2**	**30.71**	**13.93**	**10.98**	**23.25**
A/ min^{-1}	12.47	2.5	1.9	5.5	3.29	34.94
R^2	**0.8168**	**0.7321**	**0.9921**	**0.7921**	**0.8613**	**0.9963**

4.4 Rotating tube-furnace gas–solid carbonation

Comparison of free CaO and mineral CO_2 results for initial samples and for carbonated samples (hydrated (H) and non-hydrated) together with theoretical CO_{2max} values is shown on Figure 38. It can be seen that activation by hydration decreases the total free CaO levels for all three samples. BPD experiences the biggest decrease of free CaO as a result of carbonation. It is noted that the levels of activation of free CaO by hydration are higher in terms of percentage of total free CaO on BOS samples compared to BPD which shows that the hydration is more effective on both of the BOS samples. Overall mineral CO_2 levels are higher than initial levels which shows carbonation attempt with rotating tube-furnace is successful. The mineral CO_2 levels have been increased in all samples after hydration treatment, specifically for BOS1 which has higher increase in percentage compared to other samples. Values of mineral CO_2 levels of hydrated carbonated samples are compared to the theoretical CO_{2max} capacity for the following results. After hydration 72% of the theoretical CO_{2max} capacity for BOS1 and 64% for BOS2 are reached. For BPD 74% of CO_{2max} capacity is reached after hydration. The CO_2 uptake levels at the end of the rotating tube-furnace experiments shows higher percentage levels compared to the thermal analysis results. This may be due to rotation of the tube which increases gas-solid contact effecting CO_2 diffusion. According to tube furnace results selected types of BOS and BPD can be used as effective sorbents in the proposed CO_2-mineralization process, binding up to 0.15 kg CO_2 per kg of waste for BOS and 0.24 kg CO_2 per kg of waste for BPD. These results indicate that industrial application is probable as the lab-based upscaling is done effectively.

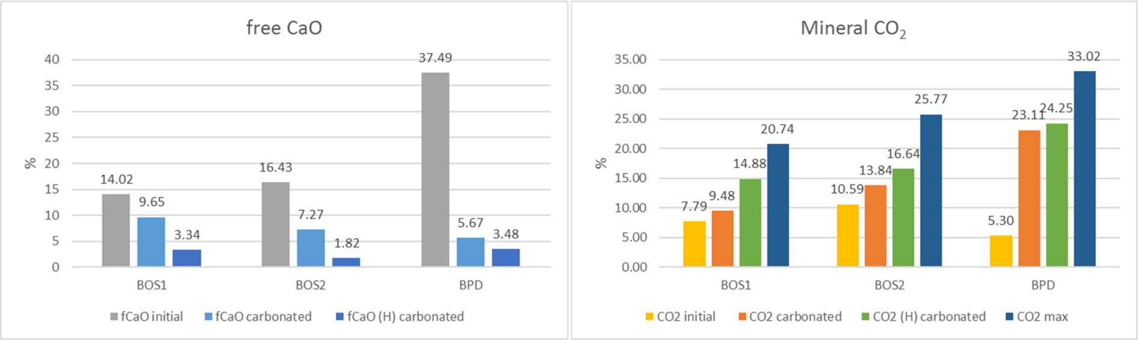

Figure 23 fCaO and mineral CO_2 changes (including theoretical CO_{2max})

4.5 FT-IR analysis

According to the FTIR analysis of the rotating tube-furnace treated samples, the intensity of portlandite peaks (3640 cm^{-1}) decreases and carbonates (872, 1417 cm^{-1}) increases after carbonation process (see Figure 24 a-f). Ca-bearing silicates (1123 cm^{-1}) play a role in carbonation reactions of BPD as their intensities also slightly decrease (see Figure 24-a). For hydrated BOS samples also the intensity of $Ca(OH)_2$ (3640 cm^{-1}) decreases after carbonation while Ca-silicates (980, 1120 cm^{-1}) does not join carbonation process (see Figure 24-c, 24-e). Peaks of the BOS spectra (1410-1415 cm^{-1}) clearly show that after hydration binding reactivity and CO_2 uptake levels BOS samples has been increased (Figure 24-d, 24-c).

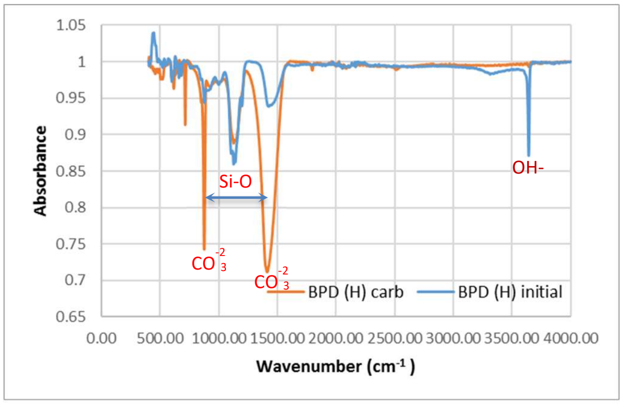

Figure 24-a FT-IR analysis BPD[H]

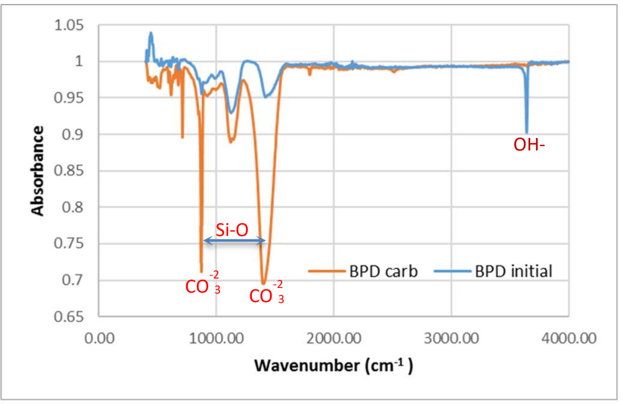

Figure 24-b FT-IR analysis BPD

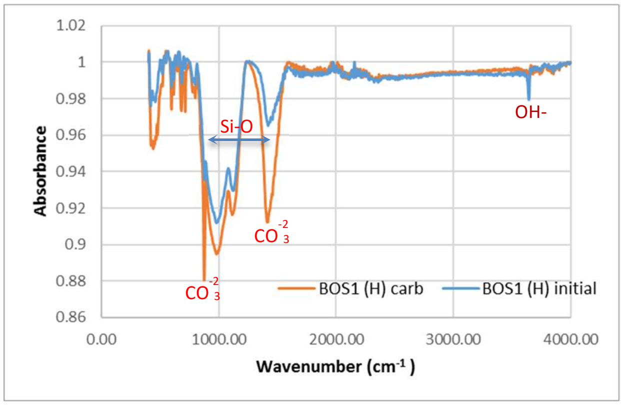

Figure 24-c FT-IR analysis BOS1[H]

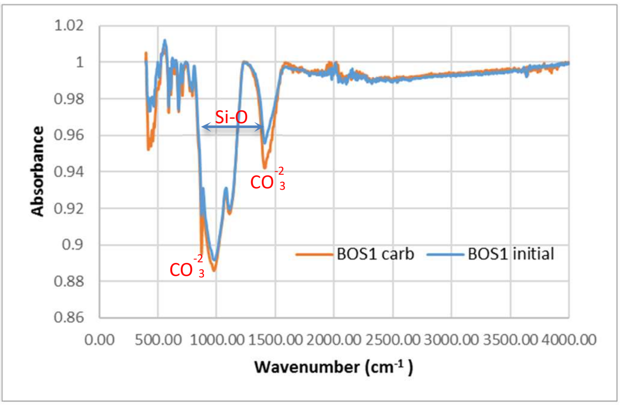

Figure 24-d FT-IR analysis BOS1

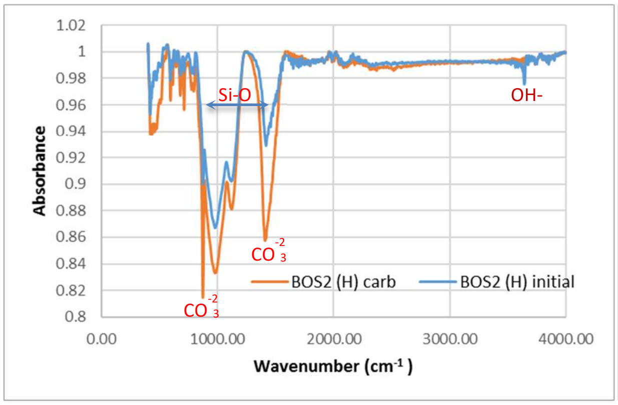

Figure 24-e FT-IR analysis BOS2[H]

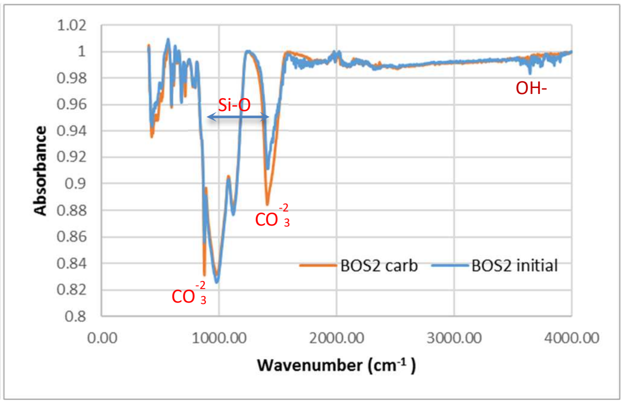

Figure 24-f FT-IR analysis BOS2

5. CONCLUSIONS

In this thesis work, direct gas-solid mineral carbonization process on industrial alkaline wastes has been employed. Series of parallel experiments were carried out with BOS and BPD under iso-thermal heating conditions by using TGA and rotating tube-furnace in order to investigate the possible applicability of the process for larger scale. The comparison of CO_2 uptake levels and reactivities during carbonation reactions of hydrated, non-hydrated and mechanically treated samples has been evaluated in the context of this thesis work.

On the basis of the obtained experimental results following conclusions can be drawn out;

- Increased temperatures show increasing CO_2 uptake capacities for all samples. Changes in CO_2 UC with increasing temperatures are more clearly expressed for the hydrated samples (1.1→1.9mg CO_2/10mg BPD(H) at 400-500°C) in comparison to non-hydrated samples (0.9→1.4mg CO_2/10mg BPD at 400-500°C).
- Activation by hydrating (liquid to solid ratio of 0.2 w/w) industrial residues CO_2 uptake potential can be increased in all samples. Approximately, 80-90% of the total theoretical CO_2 uptake has been reached in first 2-3 minutes at 500 °C and later carbonation process gradually slows down. TG tests indicate that the free CaO content could be near exhausted after 30 minutes of testing for hydrated samples at 500 °C.
- Grinding as a pretreatment has no clear positive effect on the CO_2 uptake levels even though SSA of samples were increased after the treatment. On the contrary grinding has slightly decreased the uptake capacities of studied samples which can be concluded that the mechanical treatments require further research and improved changes on the surface of the particles should also be achieved in the layer and microstructures.
- Rotating tube-furnace experiments proves the applicability of the carbonation process in larger scales containing bigger amounts of samples. In addition, by looking at mineral CO_2 and free CaO levels of carbonated samples, it is also seen that hydration has substantial positive effect on CO_2 uptake ability.
- For BOS samples Ca-Mg–silicates have almost no detected effect on carbonation under specified experimental conditions since the role of Ca-Mg–silicates in carbonation process under tested temperatures and ambient pressure without the use of additives and increased pressure could be eliminated for BOS, yet this effect is fairly small for BPD according to the obtained FTIR results showing exhausting levels of silicates.
- 41 Based on the obtained experimental findings and kinetic calculations, the most probable model for the carbonation process of non-hydrated BOS1 and BOS2 agrees with the three-

dimensional diffusion model (D3) and the most probable model for the carbonation process of the hydrated samples and non-hydrated BPD agrees with the random nucleation and nuclei growth model (A2).

- For both samples, E_a values are lower in hydrated samples which means higher rates occur during the carbonation reactions of hydrated samples.

Consequently, selected types of BOS and BPD could be used as effective sorbents in the studied CO_2-mineralization process, binding up to 0.15 kg CO_2 per kg of waste for BOS and 0.24 kg CO_2 per kg of waste for BPD. The carbonation processes of BOS and BPD and other similar mineral wastes can be optimized by hydration and temperature increase. Additionally, based on the obtained experimental findings in the context of this thesis work the effect of hydration treatment has shown that the same CO_2 uptake levels can be achieved with lower operating temperatures, thereby making the carbonation processes of similar types of industrial wastes more energy efficient and thus lowering the energy costs.

SUMMARY

The necessity to develop and invest in carbon capture technologies that can minimize the amount of CO_2 released in the environment has sparked research in innovative techniques of carbon capture. In recent years, the mineralization of gaseous CO_2 into thermodynamically stable carbonates has emerged as a promising CCS method specifically when alkaline industrial waste ashes are utilized as sorbents. The utilization of waste ashes for sequestration plays a dual role in environmental conservation, by creating avenues for recycling in the industry and by promoting the transitions towards a greener circular economy. The re-carbonated materials could be used in different industrial applications such as concrete production, therefore, the CO_2 trapped in the waste from plants can be utilized in the production of valuable goods.

The alkaline wastes of BOS and BPD generally contain free lime which makes them suitable sorbent materials for CO_2 trapping via mineral carbonation technique of CCS. In relation to the wider research on CCS in the EU - HORIZON 2020 project clean clinker production by Calcium looping process (CLEANKER), this master thesis work investigates alkaline wastes BOS and BPD as sorbents in CO_2 mineralization process in order to study the reaction kinetics and operating parameters for industrial sized scale ups, as well as to identify the effects on carbonation capacity when these sorbents undergo pre-treatment and are exposed to different temperatures.

Series of parallel experiments were carried out under iso-thermal heating conditions (50ml/min, 100%CO_2) by using TGA and rotating tube-furnace in order to test the applicability of the process for larger scale. The comparison of CO_2 uptake levels and reactivities during carbonation reactions of hydrated, non-hydrated and milled samples was evaluated in the content of this thesis work. Additionally, kinetics calculations were made based on experimental measurements and different reaction models were practiced in order to explain the mechanisms of the carbonation processes and with well-known Arhenius equation Ea and A values were obtained. The changes in sample mineralogical composition and physical characteristics were followed *via* chemical analysis, FTIR and BET methods.

Results indicates that selected types of BOS and BPD could be used as effective binders in the CO_2-mineralization systems, binding up to 0.15 kg CO_2 per kg of waste for BOS and 0.24 kg CO_2 per kg of waste for BPD. Increased temperature and hydration as pretreatment show higher CO_2 binding ability while the effect of milling has been found to be staggering and not as significant as the effect of hydration and temperature rise. According to the kinetics calculations, the calculated activation energies of hydrated samples are lower for BOS2 and BPD compared to non-hydrated samples which indicates higher rate of carbonation reactions. Hydration process demonstrates that the same CO2

uptake level can be achieved with lower temperatures, thereby making the process more energy efficient and thus lowering the costs. Consequently, the carbonation processes of similar mineral wastes can be optimized by hydration and temperature increase.

REFERENCES

1- Fossil fuel energy consumption (% of total). (n.d.). Retrieved April 1, 2019, from https://data.worldbank.org/indicator/eg.use.comm.fo.zs

2- World Energy Outlook 2017: Key Findings. (n.d.). Retrieved April 1, 2019, from https://www.iea.org/weo2017/.

3- J.G.J. Olivier, G. Janssens-Maenhout, M. Muntean, J.A.H.W. Peters. (2016) *Trends in Global CO_2 Emissions: 2016 Report*, The Hague: PblCO_2 Netherlands Environmental Assessment Agency; Ispra: European Commission Joint Research Centre

4- Lena, E. D., Spinelli, M., Gatti, M., Scaccabarozzi, R., Campanari, S., Consonni, S., Romano, M. C. (2019). Techno-economic analysis of calcium looping processes for low CO_2 emission cement plants. *International Journal of Greenhouse Gas Control, 82*, pp 244-260. doi:10.1016/j.ijggc.2019.01.005

5- IPCC, 2013: Climate Change 2013: The Physical Science Basis. Contribution of Working Group *I to the Fifth Assessment Report of the Intergovernmental Panel on Climate Change* [Stocker, T.F., D. Qin, G.-K. Plattner, M. Tignor, S.K. Allen, J. Boschung, A. Nauels, Y. Xia, V. Bex and P.M. Midgley (eds.)]. Cambridge University Press, Cambridge, United Kingdom and New York, NY, USA, p. 1535.

6- State of world population 2017 every young person's (n.d.). Retrieved from https://unfpa.org/sites/default/files/sowp/downloads/UNFPA_PUB_2017_EN_SWOP.pdf

7- U.S. Energy Information Administration - EIA - Independent Statistics and Analysis. (n.d.). Retrieved February 15, 2019, from https://www.eia.gov/todayinenergy/detail.php?id=32912

8- Oss, H. V. (n.d.). Cement Statistics and Information. Retrieved April 28, 2019, from https://minerals.usgs.gov/minerals/pubs/commodity/cement/index.html

9- Andrew, R. M (2018) Global CO_2 emissions from cement production, *Earth Syst. Sci. Data*, 10, pp. 195-217, https://doi.org/10.5194/essd-10-195-2018.

10- IPCC, 2018: Summary for Policymakers. In: Global Warming of 1.5°C. *An IPCC Special Report on the impacts of global warming of 1.5°C above pre-industrial levels and related global greenhouse gas emission pathways, in the context of strengthening the global response to the threat of climate change, sustainable development, and efforts to eradicate poverty* [Masson-Delmotte, V., P. Zhai, H.-O. Pörtner, D. Roberts, J. Skea, P.R. Shukla, A. Pirani, Moufouma-Okia, C. Péan, R. Pidcock, S. Connors, J.B.R. Matthews, Y. Chen, X. Zhou, M.I. Gomis, E. Lonnoy, Maycock, M. Tignor, and T. Waterfield (eds.)]. World Meteorological Organization, Geneva, Switzerland, pp.32

11- Cuéllar-Franca, Rosa M., and AdisaAzapagic. (2015). "Carbon Capture, Storage and Utilisation Technologies: A Critical Analysis and Comparison of Their Life Cycle Environmental Impacts." *Journal of* CO_2 *Utilization*, 9, pp. 82–102., doi:10.1016/j.jcou.2014.12.001.

12- Organization for Economic Cooperation and Development OECD, 2017.ENERGY *TECHNOLOGY PERSPECTIVES 2017: Catalysing Energy Technology Transformations*.

13- From where do we import energy and how dependent are we? (n.d.). Retrieved April 1, 2019, from https://ec.europa.eu/eurostat/cache/infographs/energy/bloc-2c.html

14- National emissions reported to the UNFCCC and to the EU Greenhouse Gas Monitoring Mechanism. (2019, March 06). Retrieved April 1, 2019, from https://www.eea.europa.eu/data-and-maps/data/national-emissions-reported-to-the-unfccc-and-to-the-eu-greenhouse-gas-monitoring-mechanism-14

15- General Principles of Climate Policy. (n.d.). Retrieved April 1, 2019, from https://www.envir.ee/en/news-goals-activities/climate/general-principles-climate-policy

16- Estonia's 2016-2030 oil shale development plan leaves extraction volume at 20 million tons. (n.d.). Retrieved April 1, 2019, from https://vm.ee/en/newsletter/estonias-2016-2030-oil-shale-development-plan-leaves-extraction-volume-20-million-tons

17- Shogenova, A., Šliaupa, S., Shogenov, K., Šliaupiene, R., Pomeranceva, R., Vaher, R., Kuusik, R. (2009). Possibilities for geological storage and mineral trapping of industrial CO_2 emissions in the Baltic region. *Energy Procedia, 1*(1), pp 2753-2760. doi:10.1016/j.egypro.2009.02.046

18- Uibu, M., &Kuusik, R. (2009). Mineral Trapping of CO_2Via Oil Shale Ash Aqueous Carbonation: Controlling Mechanism of Process Rate and Development of Continuous-Flow Reactor System. *Oil Shale, 26*(1), P 40. doi:10.3176/oil.2009.1.06

19- Uibu, M., Kuusik, R., Andreas, L., &Kirsimäe, K. (2011). The CO_2 -binding by Ca-Mg-silicates in direct aqueous carbonation of oil shale ash and steel slag. *Energy Procedia*,4, PP 925-932. doi:10.1016/j.egypro.2011.01.138

20- Rofer, C. K. (2000). *Turning a problem into a resource: Remediation and waste management at the Sillamäe site, Estonia:* Dordrecht: Kluwer Acad. Publ.

21- Scholes, C. (2019, March 12). Chemical looping: Carbons capture technology for the future. Retrieved April 1, 2019, from http://theconversation.com/chemical-looping-a-carbon-capture-technology-for-the-future-12435

22- Oexmann, J., Kather, A., Linnenberg, S., &Liebenthal, U. (2012). Post-combustion CO_2 capture: Chemical absorption processes in coal-fired steam power plants. *Greenhouse Gases: Science and Technology,* 2(2), PP 80-98. doi:10.1002/ghg.1273

23- Ho, M., & Wiley, D. (2016). Liquid absorbent-based post-combustion CO_2 capture in industrial processes. *Absorption-Based Post-combustion Capture of Carbon Dioxide, pp* 711-756. doi:10.1016/b978-0-08-100514-9.00028-7

24- Ma, J., & Yoon, R. (2015). CO_2 Mineralization in Artificial Seawater. *Novel Materials for Carbon Dioxide Mitigation Technology,*pp 363-385. doi:10.1016/b978-0-444-63259-3.00012-4

25- Zhong, D., Wang, J., Lu, Y., Li, Z., & Yan, J. (2016). Precombustion CO_2 capture using a hybrid process of adsorption and gas hydrate formation. *Energy,*102, pp 621-629. doi:10.1016/j.energy.2016.02.135

26- Hrdlicka, J., Skopec, P., Opatril, J., &Dlouhy, T. (2016). Oxyfuel Combustion in a Bubbling Fluidized Bed Combustor. *Energy Procedia, 86*, pp 116-123. doi:10.1016/j.egypro.2016.01.012

27- Ziębik, A., &Gładysz, P. (2014). Analysis of cumulative energy consumption in an oxy-fuel combustion power plant integrated with a CO_2 processing unit. *Energy Conversion and Management, 87*, pp 1305-1314. doi:10.1016/j.enconman.2014.02.048

28- Anthony, B., &Hoteit, A. (2010). Overview of Oxy-Combustion Technologies with Pure Oxygen and Chemical Looping Combustion. *Handbook of Combustion.* doi:10.1002/9783527628148.hoc090

29- Valverde, J., Sanchez-Jimenez, P., & Perez-Maqueda, L. (2014). Calcium-looping for post-combustion CO_2 capture. On the adverse effect of sorbent regeneration under CO_2. *Applied Energy,126,* pp 161-171. doi:10.1016/j.apenergy.2014.03.081

30- Huijgen, W. (2007). *Carbon dioxide sequestration by mineral carbonation: Feasibility of enhanced natural weathering as a CO_2 emission reduction technology*. S.l.

31- Seifritz, W. (1990). CO_2 disposal by means of silicates*. Nature,* 345(6275), pp. 486-486. doi:10.1038/345486b0

32- Dunsmore, H. (1992). A geological perspective on global warming and the possibility of carbon dioxide removal as calcium carbonate mineral. *Energy Conversion and Management,* 33(5-8), pp 565-572. doi:10.1016/0196-8904(92)90057-4

33- Lackner, K.S., Wendt, C.H., Butt, D.P., Joyce, E.L., Sharp, D.H.(1995). Carbon dioxide disposal in carbonate minerals. *Fuel and Energy Abstracts*, 36(6), p.457. doi:10.1016/0140-6701(95)95187-3

34- IPCC special report on carbon dioxide capture and storage. (2005). Metz, B., Davidson, O., Coninck, H., Loos, M., Meyer, L. (Eds.). UK: Cambridge University Press. P. 431.

35- Goff, F., & Lackner, K. S. (1998). Carbon Dioxide Sequestering Using Ultramafic Rocks. Environmental Geosciences,5(3), pp 89-102. doi:10.1046/j.1526-0984.1998.08014.x

36- Uibu, M.; Tamm, K.; Usta, M. C.; Žuravljova, A.; Kallas, J.; Kuusik, R.; Trikkel, A. (2019). Mineral Trapping of CO_2 for Cement Industry De-Carbonization. SSRN: Energy Research Network Conferences & Meetings: 14th Greenhouse Gas Control Technologies Conference Melbourne 21-26 October 2018 (GHGT-14). Elsevier, 1−8.

37- Huijgen W.J.J, Witkamp G.-J., Comans R.N.J.(2006) Mechanisms of aqueous wollastonite carbonation as a possible CO_2 sequestration process. – *Chemical. Engineering. Science*, 61, pp 4242–4251.

38- Bobicki, E. R., Liu, Q., Xu, Z., & Zeng, H. (2012). Carbon capture and storage using alkaline industrial wastes. *Progress in Energy and Combustion Science*, 38(2), pp 302-320. doi:10.1016/j.pecs.2011.11.002

39- Haug, T. A., Kleiv, R. A., &Munz, I. A. (2010). Investigating dissolution of mechanically activated olivine for carbonation purposes. *Applied Geochemistry*, 25(10), pp 1547-1563. doi:10.1016/j.apgeochem.2010.08.005

40- Turianicová, E., Baláž, P., Tuček, Ľ, Zorkovská, A., Zeleňák, V., Németh, Z., Kováč, J. (2013). A comparison of the reactivity of activated and non-activated olivine with CO_2. *International Journal of Mineral Processing*, pp 123, 73-77. doi:10.1016/j.minpro.2013.05.006

41- Fabian, M., Shopska, M., Paneva, D., Kadinov, G., Kostova, N., Turianicová, E., Baláž, P. (2010). The influence of attrition milling on carbon dioxide sequestration on magnesium–iron silicate. *Minerals Engineering*, 23(8), 616-620. doi:10.1016/j.mineng.2010.02.006

42- W. O'connor, D. Dahlin, G. Rush, S. Gerdemann, L. Penner, and D. Nilsen. (2004). *Aqueous mineral carbonation, mineral availability, pretreatment, reaction parametrics, and process studies in US DOE*, DOE/ARC-TR-04-002, Albany Research Centre: Albany, OR.

43- Sanna, A., Wang, X., Lacinska, A., Styles, M., Paulson, T., &Maroto-Valer, M. M. (2013). Enhancing Mg extraction from lizardite-rich serpentine for CO_2 mineral sequestration. *Minerals Engineering*, 49, pp 135-144. doi:10.1016/j.mineng.2013.05.018

44- Baláž, P., Turianicová, E., Fabián, M., Kleiv, R. A., Briančin, J., &Obut, A. (2008). Structural changes in olivine (Mg, Fe)2SiO4 mechanically activated in high-energy mills. *International Journal of Mineral Processing*, 88(1-2), pp 1-6. doi:10.1016/j.minpro.2008.04.001

45- Gerdemann, S. J., Oconnor, W. K., Dahlin, D. C., Penner, L. R., & Rush, H. (2007). Ex Situ Aqueous Mineral Carbonation. *Environmental Science & Technology*, 41(7), pp 2587-2593. doi:10.1021/es0619253

46- Lackner, K. S., Butt, D. P., & Wendt, C. H. (1997). Progress on binding CO_2 in mineral substrates. *Energy Conversion and Management*, 38, pp 259-264. doi:10.1016/s0196-8904(96)00279-8

47- Baciocchi, R., Polettini, A., Pomi, R., Prigiobbe, V., Zedwitz, V. N., & Steinfeld, A. (2006). CO_2Sequestration by Direct Gas−Solid Carbonation of Air Pollution Control (APC) Residues. Energy & Fuels, 20(5), pp 1933-1940. Doi: 10.1021/ef060135b.

48- Reddy, K. J., John, S., Weber, H., Argyle, M. D., Bhattacharyya, P., Taylor, D. T., Fahlsing, P. (2011). Simultaneous capture and mineralization of coal combustion flue gas carbon dioxide (CO_2). *Energy Procedia*, 4, pp 1574-1583. doi:10.1016/j.egypro.2011.02.027

49- Bhatia, S. K., & Perlmutter, D. D. (1983). Effect of the product layer on the kinetics of the CO_2-lime reaction. *AIChE Journal,* 29(1), pp 79-86. doi:10.1002/aic.690290111

50- Nikulshina, V., Gálvez, M., & Steinfeld, A. (2007). Kinetic analysis of the carbonation reactions for the capture of CO_2 from air via the $Ca(OH)_2$–$CaCO_3$–CaO solar thermochemical cycle. *Chemical Engineering Journa*l, 129(1-3), pp 75-83. doi:10.1016/j.cej.2006.11.003

51- M. Avrami, (1940) Kinetics of phase change. II. Transformation-time relations for random distribution of nuclei. *Journal of. Chem. Phys*. 8, pp 212–224.

52- Agrinier, P., Deutsch, A., Schärer, U., & Martinez, I. (2001). Fast back-reactions of shock-released CO 2 from carbonates: An experimental approach. *Geochimica Et Cosmochimica Acta*, 65(15), pp 2615-2632. doi:10.1016/s0016-7037(01)00617-2

53- Mess, D., Sarofim, A. F., & Longwell, J. P. (1999). Product Layer Diffusion during the Reaction of Calcium Oxide with Carbon Dioxide. *Energy & Fuels*, 13(5), pp 999-1005. doi:10.1021/ef980266f

54- Balen, K. V. (2005). Carbonation reaction of lime, kinetics at ambient temperature. *Cement and Concrete Research*, 35(4), pp 647-657. doi:10.1016/j.cemconres.2004.06.020

55- Koga, N., &Kodani, S. (2018). Thermally induced carbonation of $Ca(OH)_2$ in a CO_2 atmosphere: Kinetic simulation of overlapping mass-loss and mass-gain processes in a solid–gas system. *Physical Chemistry Chemical Physics*, 20(41), pp 26173-26189. doi:10.1039/c8cp05701j

56- Dodds WS, Stutzman, LF, and Sollami BJ. (1956). Carbon Dioxide Solubility in Water, Industrial and Engineering Chemistry. *Journal* of Chemical and Engineering Data, 1(1), pp 92-95.

57- Blencoe JG, Palmer DA, Anovitz LM, Beard JS (2004). Carbonation of metal silicates for long-term CO_2 sequestration. *Patent Number WO200409043.*

58- Chiang, Y. W., Santos, R. M., Monballiu, A., Ghyselbrecht, K., Martens, J. A., Mattos, M. L., Meesschaert, B. (2013). Effects of bioleaching on the chemical, mineralogical and morphological properties of natural and waste-derived alkaline materials. *Minerals Engineering*,48, pp 116-125. doi:10.1016/j.mineng.2012.09.004

59- Wang, X., &Maroto-Valer, M. M. (2011). Integration of CO_2 Capture and Mineral Carbonation by Using Recyclable Ammonium Salts. *ChemSusChem,* 4(9), pp 1291-1300. doi:10.1002/cssc.201000441

60- Herzog, H. (n.d.). Carbon Sequestration via Mineral Carbonation: Overview and Assessment. Retrieved April 29, 2019, from https://sequestration.mit.edu/pdf/carbonates.pdf

61- Yegulalp, T., Lackner, K., &Ziock, H. (2001). A Review of Emerging Technologies for Sustainable use of Coal for Power Generation. *International Journal of Surface Mining, Reclamation and Environment*, 15(1), pp 52-68. doi:10.1076/ijsm.15.1.52.3423

62- Zevenhoven, R., Kavaliauskaite, I., &Denafas, G. (2006). An Exergy Analysis for Mineral Carbonation, Environment, Technology, Resources. *Proceedings of the International Scientific and Practical Conference*, 1, p. 304. doi:10.17770/etr2003vol1.2025

63- Zevenhoven, R. &Teir, S. (2004) Long-term storage of CO_2 as magnesium carbonate in Finland. *3rd Annual Conference on Carbon Capture and Sequestration*, Alexandria, VA, USA.

64- Zevenhoven, R., Teir, S., &Eloneva, S. (2008). Heat optimisation of a staged gas–solid mineral carbonation process for long-term CO_2 storage. *Energy*, 33(2), pp 362-370. doi:10.1016/j.energy.2007.11.005

65- Mazzella, A., Errico, M., & Spiga, D. (2016). CO_2 uptake capacity of coal fly ash: Influence of pressure and temperature on direct gas-solid carbonation. *Journal of Environmental Chemical Engineering*, 4(4), pp 4120-4128. doi:10.1016/j.jece.2016.09.020

66- Sanna, A., Uibu, M., Caramanna, G., Kuusik, R., & Maroto-Valer, M. M. (2014). A review of mineral carbonation technologies to sequester CO_2. *Chemical Society Reviews*. doi:10.1039/C4CS00035H

67- Garcés P, Pérez Carrión M, García-Alcocel E, Payá J, Monzó J, Borrachero MV. (2008). Mechanical and physical properties of cement blended with sewage sludge ash. *Waste Management*, 28, pp 2495-502.

68- Voshell, S., Mäkelä, M., & Dahl, O. (2018). A review of biomass ash properties towards treatment and recycling. *Renewable and Sustainable Energy Reviews*, 96, pp 479-486. doi:10.1016/j.rser.2018.07.025

69- Limbachiya, M., Marrocchino, E., & Koulouris, A. (2007). Chemical–mineralogical characterisation of coarse recycled concrete aggregate. *Waste Management*, 27(2), pp 201-208. doi:10.1016/j.wasman.2006.01.005

70- Abdel-Ghani, N. T., El-Sayed, H. A., & El-Habak, A. A. (2018). Utilization of by-pass cement kiln dust and air-cooled blast-furnace steel slag in the production of some “green” cement products. *HBRC Journal*, 14(3), pp 408-414. doi:10.1016/j.hbrcj.2017.11.001

71- Gorai, B., Jana, R., &Premchand. (2003). Characteristics and utilisation of copper slag—a review. *Resources, Conservation and Recycling*, 39(4), pp 299-313. doi:10.1016/s0921-3449(02)00171-4

72- Shi, C., Meyer, C., &Behnood, A. (2008). Utilization of copper slag in cement and concrete. *Resources, Conservation and Recycling*, 52(10), pp 1115-1120. doi:10.1016/j.resconrec.2008.06.008

73- Li, J., Lü, Q., Liu, X., Zhang, S., & Liu, D. (2015). Phosphorus capacity of CaO-SiO2-Al2O3-MgO-FexO slag. *Journal of Iron and Steel Research International*, 22(5), pp 377-381. doi:10.1016/s1006-706x(15)30015-7

74- Saluja, S., Kaur, K., Goyal, S., & Bhattacharjee, B. (2019). Assessing the effect of GGBS content and aggregate characteristics on drying shrinkage of roller compacted concrete. *Construction and Building Materials,* 201, pp 72-80. doi:10.1016/j.conbuildmat.2018.12.179

75- Guo, Y., Xie, J., Zhao, J., &Zuo, K. (2019). Utilization of unprocessed steel slag as fine aggregate in normal- and high-strength concrete. *Construction and Building Materials*, 204, pp 41-49. doi:10.1016/j.conbuildmat.2019.01.178

76- Ayres, R. U., Holmberg, J., Andersson, B. (2001). Materials and the global environment: Waste mining in the 21st century. *MRS Bulletin*, 26, p.477. doi:10.1557/mrs2001.119

77- Sahu, R. C., Patel, R. K., & Ray, B. C. (2010). Neutralization of red mud using CO_2 sequestration cycle. *Journal of Hazardous Materials*, 179(1-3), pp. 28-34. doi:10.1016/j.jhazmat.2010.02.052

78- Gunning, P. J., Hills, C. D., & Carey, P. J. (2010). Accelerated carbonation treatment of industrial wastes. *Waste Management*, 30(6), pp 1081-1090. doi:10.1016/j.wasman.2010.01.005

79- Shih, Y. (2009). Thermal degradation and kinetic analysis of biodegradable PBS/multiwalled carbon nanotube nanocomposites. *Journal of Polymer Science Part B: Polymer Physics*, 47(13), pp 1231-1239. doi:10.1002/polb.21728

80- Jander, W. (1927). Reaction in the solid state at high temperature. I. Rate of reaction for an endothermic change. *Zeitschrift Für Anorganische Und Allgemeine Chemie,166*(1), 31-52. doi:10.1002/zaac.19271660105

81- Khawam, A., & Flanagan, D. R. (2006). Solid-State Kinetic Models: Basics and Mathematical Fundamentals. *ChemInform,37*(47). doi:10.1002/chin.200647223

82- Mampel, K. L. (1940). Time-vs.-amount of reaction formulas for heterogeneous reactions at the phase boundaries of solids. I. The development of the mathematical methods and the derivation of surface area-vs.-amount of reaction formulas. *Zeitschrift Für Physikalische Chemie,187A*(1). doi:10.1515/zpch-1940-18705